Available online at http://scik.org

Commun. Math. Biol. Neurosci. 2023, 2023:89

https://doi.org/10.28919/cmbn/8081

ISSN: 2052-2541

DELAY IN ECO-EPIDEMIOLOGICAL PREY-PREDATOR MODEL WITH PREDATION FEAR AND HUNTING COOPERATION

KARRAR QAHTAN AL-JUBOURI[1], RAID KAMEL NAJI[2,*]

[1]Department of Production Engineering and Metallurgy, University of Technology, Iraq

[2]Department of Mathematics, University of Baghdad, College of Science, Iraq

Abstract: It is recognized that organisms live and interact in groups, exposing them to various elements like disease, fear, hunting cooperation, and others. As a result, in this paper, we adopted the construction of a mathematical model that describes the interaction of the prey with the predator when there is an infectious disease, as well as the predator community's characteristic of cooperation in hunting, which generates great fear in the prey community. Furthermore, the presence of an incubation period for the disease provides a delay in disease transmission from diseased predators to healthy predators. This research aims to examine the proposed mathematical model's solution behavior to better understand these elements' impact on an eco-epidemic system. For all time, all solutions were proven to exist, be positive, and be uniformly bounded. The existence conditions of possible equilibrium points were determined. The stability analysis was performed for all conceivable equilibria in the presence and absence of delay. When the feedback time delays reach a critical point, the existence of Hopf bifurcation is examined. The normal form theory and the Centre manifold theorem are commonly used to investigate the dynamic properties of bifurcating cyclic solutions arising from Hopf bifurcations. Some numerical simulations were presented to validate the theoretical

*Corresponding author

E-mail address: rknaji@gmail.com

Received July 1, 2023

conclusions and understand the impact of changing the parameter values.

Keywords: eco-epidemiological model; delay; fear; hunting cooperation; stability; Hopf-bifurcation.

2020 AMS Subject Classification: 92D25, 34D20, 34K13.

1. INTRODUCTION

Although epidemiology is a significant research subject in its own right, a recent tendency has emerged to combine it with ecology to better understand species interactions in ecosystems under epidemiological variables. As a result, it gave birth to a new field: eco-epidemiology. Studying the effect of disease in the context of interspecies interactions is more realistic than studying it in isolation because no species lives in isolation in nature but interacts with a huge number of other species, either directly or indirectly. The spirit of this new route is the desire to learn about the effects of disease in prey-predator models. Anderson and May [1] were among the first to pioneer eco-epidemiological modeling. They investigated a prey-predator paradigm in which both the prey and the predator were infected. Following their pioneering work, a large number of scholars examined eco-epidemiological systems, see [2-11], which is still ongoing.

The incubation period of a disease is very important in infectious disease modeling because it determines the dynamics of disease transmission and predicts the future evolution of disease outbreaks. As a result, researchers are working to create mathematical models that more precisely reflect reality by modeling time delay. Maiti et al [12] investigated a Crowely-Martin prey-predator model in which the prey population was afflicted with illness. The nonlinear incidence rate at which vulnerable prey are infected is taken into account. Due to the existence of an incubation period, a time lag is added to convert the vulnerable prey to the infected one. Samanta et al [13] suggested and investigated a nonautonomous prey-predator model with disease in prey and a discrete-time delay for disease transmission incubation. While Hussien and Naji [14] studied the impact of the incubation time delay on disease transmission in a prey-predator system with a SI type of disease in the prey population using a nonlinear incidence rate. A modified Holling type II functional response was employed to illustrate the predation process. Further studies regarding the

impact of incubation time delay on the dynamics of eco-epidemiological systems may be found here [15-16] and the references therein.

The importance of incorporating the influence of a predator's hunting cooperation techniques in destabilizing the prey population by creating fear is one of the fundamental insights in the biological models. This is due to the fact that psychological influences can have a greater impact than direct physical predator attacks, causing the prey to migrate from more susceptible regions to less risky ones, disperse, and lose attention to key biological tasks that are part of their daily routine. For example, certain studies, such as those in [17-19], found that fear can reduce prey populations' reproductive rate and bioactivity, lowering disease transmission rates. However, it is observed that memory dependence, fear, hunting cooperation, and therapy have an impact on the fractional-order eco-epidemiological model's qualitative behavior, see [18]. On the other hand, the hunting cooperation technique affects the stability of a three-species food chain model and increases anxiety in both prey and mid-level predators, forcing them to seek refuge, see [19]. Fear of predation has many additional causes, and its prevalence is not restricted to the presence of hunting cooperation. Therefore, numerous studies have been conducted to investigate the impact of fear on the qualitative behavior and dynamics of prey and predator systems, see [20-24] and the references therein.

Based on the preceding, the study of eco-epidemiological models where there is a delay in disease transmission due to the presence of an incubation period has become a vital necessity to understand and preserve system stability by preventing the spread of infectious illness. In this study, we created a mathematical model to mimic the prey-predator system where there is an infectious sickness in the predator community with the attribute of hunting cooperation, which causes fear in the prey community as a defense against predation. The following is how this paper was structured: In Section 2, an eco-epidemiological model was established that considered infection transmission delays, hunting cooperation, and the cost of fear. Section 3 discusses solution positivity and boundedness. Section 4 addresses the presence of the model's equilibrium points. Section 5 addressed the stability of the delay model, whereas Section 6 created favorable

conditions for Hopf bifurcations. Section 7 looks into the physical properties of Hopf bifurcation limit cycles. Section 8 contains numerical simulations to validate the analytical results obtained in this paper. With a quick conclusion, the work is completed.

2. MODEL FORMULATION

This section considers the following biological hypotheses to mathematically simulate the real-world eco-epidemiological system.

- The prey population $X(t)$ has the potential to reproduce and increase naturally because of the food provided by the environment, according to the logistic growth with intrinsic growth rate $r - d_1$ and carrying capacity $\frac{r-d_1}{c}$.
- The predator can cooperate to pursue their prey, and the predation process follows the Lotka-Volterra type of functional response.
- The severity of predation causes fear in prey individuals, resulting in a decline in birth and biological functioning.
- The development of virus resistance and the unprotected connection among ecosystem individuals generates disease infection within the predator population, dividing it into two compartments $P(t) = S(t) + I(t)$, where $S(t)$ represents the susceptible individuals and $I(t)$ represents the infected individuals at the time t.
- The disease is thought to be spread through contact between $S(t)$ and $I(t)$, but it is not inherited genetically. Furthermore, an incubation period results in some lag in infectiousness at the time period τ.
- The disease leads to death in addition to the natural death of predators.

In light of the aforementioned biological hypotheses, Figure 1 depicts a block diagram depicting the above real-world system, and the set of nonlinear differential equations defining the system dynamics is written below:

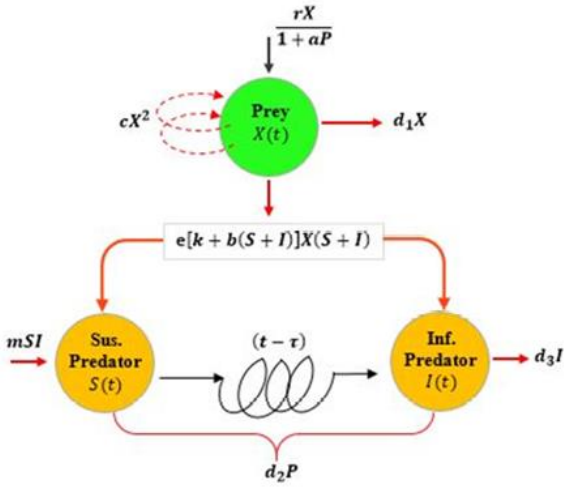

Fig. 1. Block diagram of the model

$$\begin{aligned}\frac{dX}{dt} &= \frac{rX}{1+a(S+I)} - d_1X - cX^2 - [k+b(S+I)]X(S+I) = \mathcal{F}_1(X,S,I)\\ \frac{dS}{dt} &= e[k+b(S+I)]X(S+I) - d_2S - mSI = \mathcal{F}_2(X,S,I)\\ \frac{dI}{dt} &= mS(t-\tau)\,I(t-\tau) - (d_2+d_3)I = \mathcal{F}_3(X,S,I)\end{aligned} \tag{1}$$

The biological meanings for all of the positive parameters in system (1) are shown in Table 1.

Table 1. Biological description of the system (1) parameters.

Parameter	***Biological Identification***
r	The birth rate of the prey population
a	Predation fear rate
d_1	The natural death rate of prey
d_2	The natural death rate of susceptible predators
d_3	The mortality rate of infected predators as a result of the epidemic
c	Coefficient intraspecific competition among prey
k	The attack rate of predators
b	A cooperative hunting level of predators
e	The conversion rate of prey's biomass into predator's biomass
m	Infection rate
τ	The time lag in transmission of infection

The following are the system's (1) initial conditions:

$$\begin{aligned} X(t) &= \psi_1(t) \\ S(t) &= \psi_2(t) \\ I(t) &= \psi_3(t) \end{aligned} \tag{2}$$

where $\psi = (\psi_1, \psi_2, \psi_3)^T \in C_+ = C_+([-\tau, 0], \mathbb{R}^3_+)$, such that $\psi_i(t) \geq 0$ $(i = 1,2,3)$, $\forall\, t \in [-\tau, 0]$, with $\|\psi\| = \underset{-\tau \leq t \leq 0}{Sup} \{ |\psi_1(t)|, |\psi_2(t)|, |\psi_3(t)| \}$.

In addition, the functions $\mathcal{F}_i$ $(i = 1,2,3)$ are obviously continuous and meet the local Lipschitz condition on C_+. As a result, using the fundamental theorem of functional differential equations [25] ensures that system (1) has a unique solution that meets the initial conditions (2).

3. POSITIVITY AND BOUNDEDNESS

Before proceeding with the study, confirm that the proposed model is biologically sound. Consequently, in this section, we present the following theorem, which explores the positivity and boundedness of the system.

Theorem 1. All system (1) solutions starting in $\mathbb{R}^3_+$ remain positive and bounded forever.

Proof. From the prey equation of system (1), we have

$$\frac{dX}{dt} = X\left(\frac{r}{1+a(S+I)} - d_1 - cX - \big(k + b(S+I)\big)(S+I)\right)$$

This yield:

$$X(t) = X(0)\, exp\left\{\int_0^t \left(\frac{r}{1+a\big(S(\varepsilon)+I(\varepsilon)\big)} - d_1 - cX(\varepsilon) - \Big(k + b\big(S(\varepsilon)+I(\varepsilon)\big)\Big)\big(S(\varepsilon)+I(\varepsilon)\big)\right) d(\varepsilon)\right\},$$

which implies $X(t) > 0$ for all time $t \geq 0$ whenever $X(0) > 0$.

The positivity of predator species is now demonstrated, from the susceptible equation of system (1), we have

$$\frac{dS}{dt} \geq -S(d_2 + mI).$$

By solving this inequality, we obtain

$$S(t) \geq S(0)\, exp\left\{-\int_0^t \big(d_2 + mI(\varepsilon)\big)\, d(\varepsilon)\right\} > 0\,,$$

whenever $S(0) > 0$ for all time $t \geq 0$.

Similarly, from the infected equation of system (1), we have $I(t) > 0$ for all time $t \geq 0$ whenever $I(0) > 0$. Hence, solutions of the system (1) are positive.

Next, regarding the boundedness of the solutions. From the prey equation of system (1), we can obtain

$$\frac{dX}{dt} \leq \frac{rX}{1+a(S+I)} - d_1X - cX^2 \leq (r - d_1)X - cX^2$$

which implies

$$\lim_{t \to \infty} sup\, X(t) \leq \frac{r-d_1}{c}$$

To guarantee that the prey species do not extinct, the condition $r > d_1$ should be met. Hence, for small enough $\delta > 0$, there exists $t^* > 0$ such that

$$X(t) \leq \frac{r-d_1}{c} + \delta, \text{ for } t > t^*.$$

Now we consider, $V(t) = X(t-\tau) + \frac{1}{e}S(t-\tau) + I(t)$ and $t > t^* + \tau$. Then, we have

$$\begin{aligned}
\frac{dV}{dt} &= \frac{rX(t-\tau)}{1+a\left(S(t-\tau)+I(t-\tau)\right)} - d_1X(t-\tau) - cX(t-\tau)^2 - \frac{d_2}{e}S(t-\tau) - (d_2+d_3)I \\
&\leq (r-d_1)X(t-\tau) - \frac{d_2}{e}S(t-\tau) - (d_2+d_3)I \\
&\leq 2\,(r-d_1)X(t-\tau) - \mathcal{B}V(t) \\
&\leq\ 2\,(r-d_1)\left(\frac{r-d_1}{c} + \delta\right) - \mathcal{B}V(t),
\end{aligned}$$

where $\mathcal{B} = min\{(r-d_1), d_2\,, (d_2+d_3)\}$. This yield

$$\lim_{t \to \infty} sup\, V(t) \leq \frac{2}{\mathcal{B}}\,(r-d_1)\left(\frac{r-d_1}{c} + \delta\right).$$

Hence, all the solutions of system (1) are bounded.

4. THE SYSTEM'S (1) EQUILIBRIA

It is worth noting that system (1) has no more than four non-negative equilibrium points. The followings are the equilibrium points and their existence conditions:

The total extinction equilibrium point (TEE), $E_0 = (0,0,0)$, always exists.

The axial equilibrium point (AE), $E_1 = (\tilde{X}, 0,0)$, where $\tilde{X} = \frac{r-d_1}{c}$, which always exists.

The infected predator-free equilibrium (IPFE), $E_2 = (\hat{X}, \hat{S}, 0)$, where $\hat{X} = \frac{d_2}{e(k+b\hat{S})}$ while $\hat{S}$ is the positive root of the equation:

$$A_1 S^4 + A_2 S^3 + A_3 S^2 + A_4 S + A_5 = 0, \tag{3}$$

where

$$A_1 = -ab^2 e.$$
$$A_2 = -eb(2ak + b).$$
$$A_3 = -e(abd_1 + ak^2 + 2kb).$$
$$A_4 = erb - (ebd_1 + eakd_1 + acd_2 + ek^2).$$
$$A_5 = erk - (ekd_1 + cd_2).$$

Obviously, equation (3) has a unique positive root and hence IPFE exists uniquely, provided that the following condition is met.

$$A_5 > 0. \tag{4}$$

The positive equilibrium (PE), $E^* = (X^*, S^*, I^*)$, where

$$\left.\begin{array}{c} X^* = \frac{(d_2+mI^*)S^*}{ekS^*+ebS^{*2}+2beS^*I^*+ebI^{*2}+ekI^*} \\ S^* = \frac{d_2+d_3}{m} \end{array}\right\}, \tag{5}$$

while I^* is the positive root of the following equation:

$$B_1 I^5 + B_2 I^4 + B_3 I^3 + B_4 I^2 + B_5 I + B_6 = 0, \tag{6}$$

where

$$B_1 = -ab^2 e,$$
$$B_2 = -(5ab^2 eS^* + 2abek + b^2 e),$$
$$B_3 = -\left(abed_1 + aek^2 + 8abekS^* + 10ab^2 eS^{*2} + 2bek + 4eb^2 S^* + eb^2 S^{*3}\right),$$
$$B_4 = eb(r - d_1)\left[3abed_1 S^* + 6bekS^* + 10abekS^{*2} + 3aek^2 S^* + 6b^2 eS^{*2} + 10ab^2 eS^{*3} + 2abekS^* + ad_1 ek + ek^2\right],$$
$$B_5 = e\,(r - d_1)(k + 2bS^*) - [2aed_1 kS^* + 2ek^2 S^* + (cm + acmS^* + acd_1 + acm)S^* + 3abed_1 S^{*2} + 3aek^2 S^{*2} + 6bekS^{*2} + 8abekS^{*3} + 3b^2 eS^{*3} + 5ab^2 eS^{*4}],$$
$$B_6 = eS^*\,(r - d_1)(k + bS^*) - [5ab^2 eS^* + 2abek + eb^2].$$

It is worth noting that equation (6) has a unique positive root; hence, the PE exists uniquely if the

following conditions are met.

$$B_i > 0\ ;\ i = 5,6. \tag{7}$$

5. STABILITY ANALYSIS

One of the strategies to analyze the nature of the stability of the equilibrium is through linearization. Accordingly, define $\tilde{E} = (\tilde{X}, \tilde{S}, \tilde{I})$ as an arbitrary equilibrium point of the system (1). Further, let $X(t) = W_1(t) + \tilde{X}$, $S(t) = W_2(t) + \tilde{S}$, and $I(t) = W_3(t) + \tilde{I}$. Then, the linearized system at $\tilde{E}$ can be expressed as follows:

$$\begin{aligned} \dot{W}_1(t) &= a_{11}\, W_1(t) + a_{12}\, W_2(t) + a_{13}\, W_3(t), \\ \dot{W}_2(t) &= a_{21}\, W_1(t) + a_{22}\, W_2(t) + a_{23}\, W_3(t), \\ \dot{W}_3(t) &= b_{32}\, W_2(t-\tau) + a_{33}\, W_3 + b_{33}\, W_3(t-\tau), \end{aligned} \tag{8}$$

where

$$a_{11} = \frac{r}{1+a(\tilde{S}+\tilde{I})} - \left(d_1 + 2c\tilde{X} + k\tilde{S} + b\tilde{S}^2 + 2b\tilde{S}\tilde{I} + b\tilde{I}^2 + k\tilde{I}\right),$$

$$a_{12} = -\left(\frac{ar\tilde{X}}{\left(1+a(\tilde{S}+\tilde{I})\right)^2} + \left(k\tilde{X} + 2b\tilde{X}\tilde{S} + 2b\tilde{X}\tilde{I}\right)\right) = a_{13},$$

$$a_{21} = ek\tilde{S} + eb\tilde{S}^2 + 2eb\tilde{S}\tilde{I} + eb\tilde{I}^2 + ek\tilde{I},$$

$$a_{22} = ek\tilde{X} + 2eb\tilde{X}\tilde{S} + 2eb\tilde{X}\tilde{I} - d_2,$$

$$a_{23} = ek\tilde{X} + 2eb\tilde{X}\tilde{S} + 2eb\tilde{X}\tilde{I} - m\tilde{S},$$

$$b_{32} = m\tilde{I},\ a_{33} = -(d_2 + d_3),\ b_{33} = m\tilde{S}.$$

Consequently, the characteristic equation of the system (1) at $\tilde{E}$ can be determined from the following characteristic equation:

$$\begin{vmatrix} a_{11} - \lambda & a_{12} & a_{13} \\ a_{21} & a_{22} - \lambda & a_{23} \\ 0 & b_{32}\, e^{-\lambda\tau} & \left(a_{33} + b_{33}\, e^{-\lambda\tau}\right) - \lambda \end{vmatrix} = 0. \tag{9}$$

Next, the behavior of the each equilibrium point of system (1) for all $\tau \geq 0$, is analyzed in the following theorems:

Theorem 2. The TEE of the system (1) is unstable saddle point when $d_1 < r$.

Proof: The characteristic equation (9) at E_0 becomes

$$[(r-d_1)-\lambda][-d_2-\lambda][-(d_2+d_3)-\lambda]=0. \tag{10}$$

Obviously, the equation (10) has one positive root $\lambda_1=(r-d_1)$, with two negative roots $\lambda_2=-d_2$, and $\lambda_3=-(d_2+d_3)$. Hence, the (TEE) E_0 is unstable saddle point. Otherwise, when $r-d_1<0$, then prey population will be extinct and hence, the system completely collapses and the solution approaches TEE.

Theorem 3. The AE of the system (1) is locally asymptotically stable if and only if the following condition is met.

$$\frac{ek(r-d_1)}{c}-d_2<0. \tag{11}$$

Otherwise, the AE is unstable saddle point.

Proof: For the equilibrium point AE that given by E_1, the characteristic equation (9) can be expressed as:

$$(-(r-d_1)-\lambda)\left(\left(ek\frac{(r-d_1)}{c}-d_2\right)-\lambda\right)(-(d_2+d_3)-\lambda)=0. \tag{12}$$

Clearly, the equation (12) have three real roots given by

$$\lambda_1=-(r-d_1)<0,\ \lambda_2=ek\frac{(r-d_1)}{c}-d_2, \text{ and } \lambda_3=-(d_2+d_3)<0.$$

Thus, condition (11) guarantees that, AE is locally asymptotically stable. Otherwise, E_1 is unstable saddle point due to existence of negative eigenvalues.

Theorem 4. Assume that the following condition holds.

$$\left.\begin{array}{c}-(\hat{a}_{11}+\hat{a}_{22})>0\\ \hat{a}_{11}\hat{a}_{22}-\hat{a}_{12}\hat{a}_{21}>0\end{array}\right\} \tag{13}$$

Then, the IPFE of the system (1) is locally asymptotically stable for all $\tau\geq 0$ if and only if the following condition holds.

$$m\hat{S}<(d_2+d_3), \tag{14}$$

It is unstable saddle point for all $0\leq\tau<\tau_c=\frac{1}{\sqrt{(m\hat{S})^2-(d_2+d_3)^2}}arccos\left(\frac{d_2+d_3}{m\hat{S}}\right)$ if the condition (14) is replaced by the following condition

$$(d_2+d_3)<m\hat{S}. \tag{15}$$

Where all the new symbols are defined in the proof.

Proof: For IPFE that given by E_2, the characteristic equation (9) become

$$\begin{vmatrix} \hat{a}_{11}-\lambda & \hat{a}_{12} & \hat{a}_{13} \\ \hat{a}_{21} & \hat{a}_{22}-\lambda & \hat{a}_{23} \\ 0 & 0 & \left(\hat{a}_{33}+\hat{b}_{33}\,e^{-\lambda\tau}\right)-\lambda \end{vmatrix}=0,$$

which gives

$$[\lambda^2-(\hat{a}_{11}+\hat{a}_{22})\lambda+(\hat{a}_{11}\hat{a}_{22}-\hat{a}_{12}\hat{a}_{21})]\left[\left(\hat{a}_{33}+\hat{b}_{33}\,e^{-\lambda\tau}\right)-\lambda\right]=0, \tag{16}$$

where

$$\hat{a}_{11}=\frac{r}{1+a\hat{S}}-\left(d_1+2c\hat{X}+k\hat{S}+b\hat{S}^2\right),\ \hat{a}_{12}=\hat{a}_{13}=-\left(\frac{ar\hat{X}}{(1+a\hat{S})^2}+\left(k\hat{X}+2b\hat{X}\hat{S}\right)\right),$$

$$\hat{a}_{21}=ek\hat{S}+eb\hat{S}^2,\ \hat{a}_{22}=ek\hat{X}+2eb\hat{X}\hat{S}-d_2,\ \hat{a}_{23}=ek\hat{X}+2eb\hat{X}\hat{S}-m\hat{S},$$

$$\hat{a}_{33}=-(d_2+d_3),\ \hat{b}_{33}=m\hat{S}.$$

Consequently, due to Routh-Hurwitz criterion, a quadratic factor in equation (16), has two eigenvalues with negative real parts if the condition (13) is met. While, the transcendental factor in equation (16) is subject to proposition (1) [26], which gives that:

If condition (14) holds, then all the roots of the transcendental equation have negative real parts for any $\tau \geq 0$. Thus, the IPFE that given by E_2 is locally asymptotically stable.

However, if condition (15) holds then the transcendental equation have positive real parts roots for $0 \leq \tau < \tau_c$. Hence, the IPFE is a saddle point. This is complete the proof.

Theorem 5. Assume that the following set of requirements are satisfied,

$$\left.\begin{array}{c} a_{11}^*<0, a_{22}^*<0 \\ a_{23}^*<0, a_{33}^*+b_{33}^*<0 \\ a_{23}^*(a_{22}^*+a_{33}^*+b_{33}^*)+a_{13}^*a_{21}^*>0 \end{array}\right\} \tag{17}$$

Then, E^* is locally asymptotically stable for $\tau=0$ and becomes unstable for $\tau \geq \tau^{\wedge}$ for a critical value $\tau^{\wedge}>0$ if in addition to the set (17) the following requirement is met

$$D_3^2-D_6^2<0. \tag{18}$$

where D_i's are specified in the proof.

Proof: For the PE that given by E^*, the characteristic equation (9) will be written as:

$$\begin{vmatrix} a_{11}^*-\lambda & a_{12}^* & a_{13}^* \\ a_{21}^* & a_{22}^*-\lambda & a_{23}^* \\ 0 & b_{32}^*\,e^{-\lambda\tau} & \left(a_{33}^*+b_{33}^*\,e^{-\lambda\tau}\right)-\lambda \end{vmatrix}=0,$$

where

$$a_{11}^* = \frac{r}{1+a(S^*+I^*)} - \left(d_1 + 2cX^* + kS^* + bS^{*2} + 2bS^*I^* + bI^{*2} + kI^*\right),$$

$$a_{12}^* = -\left(\frac{arX^*}{\left(1+a(S^*+I^*)\right)^2} + (kX^* + 2bX^*S^* + 2bX^*I^*)\right) = a_{13}^*,$$

$$a_{21}^* = ekS^* + ebS^{*2} + 2ebS^*I^* + ebI^{*2} + ekI^*,$$

$$a_{22}^* = ekX^* + 2ebX^*S^* + 2ebX^*I^* - d_2,$$

$$a_{23}^* = ekX^* + 2ebX^*S^* + 2ebX^*I^* - mS^*,\ a_{33}^* = -(d_2 + d_3),$$

$$b_{32}^* = mI^*,\ b_{33}^* = mS^*.$$

Direct computation leads to have the following characteristic equation of the system (1) at E^*:

$$P(\lambda) - Q(\lambda)e^{-\lambda\tau} = 0, \tag{19}$$

where

$$P(\lambda) = \lambda^3 + D_1\lambda^2 + D_2\lambda + D_3.$$

$$Q(\lambda) = D_4\lambda^2 + D_5\lambda + D_6.$$

With

$$D_1 = -(a_{11}^* + a_{22}^* + a_{33}^*).$$

$$D_2 = a_{11}^*a_{22}^* + a_{11}^*a_{33}^* + a_{22}^*a_{33}^* - a_{12}^*a_{21}^*.$$

$$D_3 = -(a_{11}^*a_{22}^* - a_{12}^*a_{21}^*)a_{33}^*.$$

$$D_4 = b_{33}^*.$$

$$D_5 = -(a_{11}^*b_{33}^* + a_{22}^*b_{33}^* - a_{23}^*b_{32}^*).$$

$$D_6 = a_{11}^*a_{22}^*b_{33}^* + a_{13}^*a_{21}^*b_{32}^* - a_{11}^*a_{23}^*b_{32}^* - a_{12}^*a_{21}^*b_{33}^*.$$

Consequently, the eigenvalues of the characteristic equation (19) can be classified in two cases:

For $\boldsymbol{\tau = 0}$, the equation (19) is rewritten as:

$$\lambda^3 + (D_1 - D_4)\lambda^2 + (D_2 - D_5)\lambda + (D_3 - D_6) = 0, \tag{20}$$

where

$$D_1 - D_4 = -(a_{11}^* + a_{22}^* + a_{33}^* + b_{33}^*).$$

$$D_2 - D_5 = a_{11}^*a_{22}^* + a_{11}^*a_{33}^* + a_{22}^*a_{33}^* - a_{12}^*a_{21}^* + a_{11}^*b_{33}^* + a_{22}^*b_{33}^* - a_{23}^*b_{32}^*.$$

$$D_3 - D_6 = -(a_{11}^*a_{22}^* - a_{12}^*a_{21}^*)(a_{33}^* + b_{33}^*) - (a_{13}^*a_{21}^* - a_{11}^*a_{23}^*)b_{32}^*.$$

Moreover

$$(D_1 - D_4)(D_2 - D_5) - (D_3 - D_6) = -(a_{11}^* a_{22}^* - a_{12}^* a_{21}^*)(a_{11}^* + a_{22}^*) \\ -(a_{11}^* + a_{22}^*)^2(a_{33}^* + b_{33}^*) - (a_{11}^* + a_{22}^*)(a_{33}^* + b_{33}^*)^2 \\ +[a_{23}^*(a_{22}^* + a_{33}^* + b_{33}^*) + a_{13}^* a_{21}^*]\, b_{32}^*$$

Now, direct computation shows that the set of conditions (17) guarantees that all the eigenvalues of characteristic equation (20) have negative real parts. Hence according the Routh–Hurwitz criterion, E^* is locally asymptotically stable.

In the second case, when $\boldsymbol{\tau > 0}$, the equation (19) has infinitely many roots. Thus, we claim that $\lambda(\tau) = \alpha(\tau) + i\beta(\tau)$ represents the general eigenvalue of equation (19). Then substituting this eigenvalue in the equation (19), isolating real and imaginary parts yields:

$$\alpha^3 - 3\alpha\beta^2 + \alpha^2 D_1 - \beta^2 D_1 + \alpha D_2 + D_3 = [(\alpha^2 D_4 - \beta^2 D_4 + \alpha D_5 + D_6) \\ \cos(\beta\tau) + (2\alpha\beta D_4 + \beta D_5)\sin(\beta\tau)]\, e^{-\alpha\tau} \tag{21}$$

$$3\alpha^2\beta - \beta^3 + 2\alpha\beta D_1 + \beta D_2 = [(2\alpha\beta D_4 + \beta D_5)\cos(\beta\tau) \\ -\big((\alpha^2 - \beta^2)D_4 + \alpha D_5 + D_6\big)\, sin(\beta\tau)]e^{-\alpha\tau} \tag{22}$$

Now, since the stability of the point E^* is changed when the real part of the eigenvalues $\lambda(\tau)$ crosses the imaginary axis from the left to the right at a specific value of $\tau = \tau^{\wedge}$ with $\beta(\tau^{\wedge}) > 0$ to be exist. Therefore, substituting $\alpha = 0$ in the equations (21)-(22), yields:

$$(D_6 - D_4\beta^2)\cos(\beta\tau) + D_5\,\beta\sin(\beta\tau) = D_3 - D_1\,\beta^2. \tag{23}$$

$$D_5\,\beta\cos(\beta\tau) - (D_6 - D_4\beta^2)\sin(\beta\tau) = D_2\,\beta - \beta^3. \tag{24}$$

By squaring and adding (23) and (24), it is arrived the following algebraic equation of β:

$$\beta^6 + (D_1^2 - 2D_2 - D_4^2)\beta^4 + (D_2^2 - 2D_1D_3 + 2D_4D_6 - D_5^2)\beta^2 + (D_3^2 - D_6^2) = 0. \tag{25}$$

Let $= \beta^2$, then the equation (25) is transform to:

$$Z^3 + \varphi_1 Z^2 + \varphi_2 Z + \varphi_3 = 0, \tag{26}$$

where

$$\varphi_1 = D_1^2 - 2D_2 - D_4^2$$

$$\varphi_2 = D_2^2 - 2D_1D_3 + 2D_4D_6 - D_5^2.$$

$$\varphi_3 = D_3^2 - D_6^2.$$

Obviously, condition (18) guarantees that equation (26), and hence (25), has at least one positive root $\beta(\tau^{\wedge}) = \sqrt{Z}$. Thus, for $\tau^{\wedge} \leq \tau$, the equation (19) has roots with the positive real part that

makes E^* unstable.

Moreover, it is well known that the equation (26) possesses three roots represented by Z_1, Z_2, and Z_3. At least one of them, say $Z_k; k = 1, or\ 2, or\ 3$, will be positive provided that conditions (17)-(18) are satisfied. Hence, the equation (25) will have a positive root $\beta_0 = \sqrt{Z_k}$. Hence, based on the equations (23) - (24), if $Z_k > 0$, the corresponding $\tau^{\wedge} > 0$, can be determined such that

$$\tau_j^{\wedge} = \frac{1}{\beta_0} arccos\left(\frac{(D_1D_4 - D_5)\,\beta_0^4 + (D_2D_5 - (D_1D_6 + D_3D_4))\,\beta_0^2 + D_3D_6}{D_4^2\,\beta_0^4 + (D_5^2 - 2D_4D_6)\,\beta_0^2 + D_6^2}\right) + \frac{2j\pi}{\beta_0}, \text{ j = 0,1,2, …} \qquad (27)$$

where $\tau^{\wedge} = \min \tau_j^{\wedge}$. In order to complete the proof criteria for $\tau = \tau^{\wedge}$, we will explore this in the next section.

6. HOPF BIFURCATION DYNAMICS

In this section, the dynamics behavior of the system (1) around the PE at $\tau = \tau^{\wedge}$ is investigated.

Theorem 6. The system (1) will lose its stability and undergo a Hopf bifurcation at E^* when $\tau = \tau^{\wedge}$, if the following condition is met

$$H(\beta_0)\,F(\beta_0) - I(\beta_0)\,G(\beta_0) \neq 0, \qquad (28)$$

where H, F, I, and G are established in proof.

Proof: According to the theorem (5), system (1) losses its stability at E^* when $\tau = \tau^{\wedge}$, and the system has a complex conjugate eigenvalues $\lambda(\tau) = \alpha(\tau) \pm i\beta(\tau)$, where τ in the neighborhood of $\tau^{\wedge}$ with $\lambda(\tau^{\wedge}) = \pm i\beta_0$, and $\beta_0 > 0$. Hence the first requirements of the occurrence of Hopf bifurcation around E^* is satisfied. Therefore, the system (1) is said to be undergo Hopf bifurcation if the transversality criterion $\frac{d}{d\tau} Re\,\{\lambda(\tau)\}\Big|_{\tau = \tau^{\wedge}} \neq 0$ is met. Now, substituting $\lambda(\tau) = \alpha(\tau) + i\beta(\tau)$ in the equation (19), and then set $\alpha(\tau) = 0$ after separating the real and imaginary components gives that:

$$\begin{aligned} F(\beta)\,\frac{d\alpha}{d\tau} + G(\beta)\,\frac{d\beta}{d\tau} &= H(\beta), \\ -G(\beta)\,\frac{d\alpha}{d\tau} + F(\beta)\,\frac{d\beta}{d\tau} &= I(\beta), \end{aligned} \qquad (29)$$

where

$$\begin{aligned} F(\beta) &= D_2 - 3\beta^2 + \{(D_6 - \beta^2 D_4)\,\tau - D_5\}\cos(\beta\tau) + \beta(\tau D_5 - 2D_4)\sin(\beta\tau), \\ G(\beta) &= -2\beta D_1 + \beta(2D_4 - \tau D_5)\cos(\beta\tau) + \{(D_6 - \beta^2 D_4)\,\tau - D_5\}\sin(\beta\tau), \end{aligned}$$

$$H(\beta) = \beta^2 D_5 \cos(\beta\tau) + \beta(\beta^2 D_4 - D_6)\sin(\beta\tau),$$
$$I(\beta) = \beta(D_6 - \beta^2 D_4)\cos(\beta\tau) + \beta^2 D_5 \sin(\beta\tau).$$

Solving the linear algebraic system (29) for $\frac{d\alpha}{d\tau}$, gives that

$$\frac{d\alpha}{d\tau}\Big|_{\substack{\tau=\tau^{\wedge} \\ \beta=\beta_0}} = \frac{H(\beta_0)\,F(\beta_0) - I(\beta_0)\,G(\beta_0)}{F(\beta_0)^2 + G(\beta_0)^2}$$

Obviously, $\frac{d}{d\tau} Re\,\{\lambda(\tau)\}\Big|_{\substack{\tau=\tau^{\wedge} \\ \beta=\beta_0}} \neq 0$, provided that condition (28) is satisfied. As a result, a Hopf Bifurcation occurs at $\tau = \tau^{\wedge}$. This ends the proof.

7. STABILITY AND DIRECTION OF HOPF BIFURCATION

In this section, the dynamical features of bifurcating cyclic solutions emerging from Hopf bifurcations are widely analyzed by utilizing the normal form theory and Centre manifold reduction introduced by [27].

Let us rewritten $W_1(t) = X - X^*,\ W_2(t) = S - S^*,\ W_3(t) = I - I^*, and\ \eta = \tau - \tau^{\wedge}$, where $\eta \in \mathbb{R}$ and at $\eta = 0$ gives the value of Hopf bifurcation. After rescaling $t \to {}^{t}/_{\tau}$, system (1) can be express as

$$\dot{W}(t) = T_\eta(W_t) + F(\eta, W_t), \tag{30}$$

where $W(t) = \big(W_1(t), W_2(t), W_3(t)\big)^T \in \mathbb{R}^3$, $T_\eta : C \to \mathbb{R}^3$, $F : \mathbb{R} \times C \to \mathbb{R}^3$, and $C = C([-1, 0], \mathbb{R}^3_+)$. Thus, for $\varphi = (\varphi_1, \varphi_2, \varphi_3)^T \in C$, we have:

$$T_\eta(\varphi) = (\tau^{\wedge} + \eta)\big(A\,\varphi(0) + B\,\varphi(-1)\big). \tag{31}$$

and

$$F(\eta, \varphi) = (\tau^{\wedge} + \eta)\begin{pmatrix} F_1 \\ F_2 \\ F_3 \end{pmatrix}. \tag{32}$$

With

$$A = \begin{pmatrix} f_{100}^{(1)} & f_{010}^{(1)} & f_{001}^{(1)} \\ f_{100}^{(2)} & f_{010}^{(2)} & f_{001}^{(2)} \\ 0 & 0 & f_{100}^{(3)} \end{pmatrix} = \begin{pmatrix} a_{11} & a_{12} & a_{13} \\ a_{21} & a_{22} & a_{23} \\ 0 & 0 & a_{33} \end{pmatrix},$$

and

$$B = \begin{pmatrix} 0 & 0 & 0 \\ 0 & 0 & 0 \\ 0 & f_{010}^{(3)} & f_{001}^{(3)} \end{pmatrix} = \begin{pmatrix} 0 & 0 & 0 \\ 0 & 0 & 0 \\ 0 & b_{32} & b_{33} \end{pmatrix}.$$

Here, the symbols a_{ij}, and b_{ij} indicated in the equation (8). Moreover,

$$F_1 = \sum_{i+l+j\geq 2} \frac{1}{i!\, l!\, j!} f_{ilj}^{(1)} \varphi_1^i(0)\, \varphi_2^l(0)\, \varphi_3^j(0)$$

$$F_2 = \sum_{i+l+j\geq 2} \frac{1}{i!\, l!\, j!} f_{ilj}^{(2)} \varphi_1^i(0)\, \varphi_2^l(0)\, \varphi_3^j(0)$$

$$F_3 = \sum_{j+k+m\geq 2} \frac{1}{j!\, k!\, m!} f_{ilj}^{(3)} \varphi_3^j(0)\, \varphi_2^k(-1)\, \varphi_3^m(-1)$$

where $i, l, j, k, m \geq 0$, we define

$$\begin{aligned} \boldsymbol{f^{(1)}(\varphi_1, \varphi_2, \varphi_3)} &= \frac{r_1(\varphi_1 + X^*)}{1 + a(\varphi_2 + \varphi_3 + S^* + I^*)} \\ &-[c\varphi_1^2 + (d_1 + 2cX^* + kS^* + b(S^*)^2 + 2bS^*I^* + b(I^*)^2 + kI^*)\varphi_1 \\ &+(k + 2bS^* + 2bI^*)\varphi_1\varphi_2 + (k + 2bS^* + 2bI^*)\varphi_1\varphi_3 + 2b\varphi_1\varphi_2\varphi_3 \\ &+b\varphi_1\varphi_2^2 + b\varphi_1\varphi_3^2 + bX^*\varphi_2^2 + (kX^* + 2bX^*S^* + 2bX^*I^*)\varphi_2 \\ &+2bX^*\varphi_2\varphi_3 + bX^*\varphi_3^2 + (kX^* + 2bX^*S^* + 2bX^*I^*)\varphi_3 \\ &+(d_1X^* + c(X^*)^2 + kX^*S^* + bX^*(S^*)^2 + 2bX^*S^*I^* + bX^*(I^*)^2 + kX^*I^*)] \end{aligned}$$

$$\begin{aligned} \boldsymbol{f^{(2)}(\varphi_1, \varphi_2, \varphi_3)} &= (ekS^* + eb(S^*)^2 + eb(I^*)^2 + 2ebS^*I^* + ekI^*)\varphi_1 \\ &+(ek + 2ebS^* + 2ebI^*)\varphi_1\varphi_2 + (ek + 2ebI^* + 2ebS^*)\varphi_1\varphi_3 \\ &+2eb\varphi_1\varphi_2\varphi_3 + eb\varphi_1\varphi_2^2 + eb\varphi_1\varphi_3^2 + ebX^*\varphi_2^2 \\ &+\big(ekX^* + 2ebX^*S^* + 2ebX^*I^* - (d_2 + mI^*)\big)\varphi_2 + (2ebX^* - m)\varphi_2\varphi_3 \\ &+ebX^*\varphi_3^2 + (ekX^* + 2ebX^*S^* + 2ebX^*I^* - mS^*)\varphi_3 \\ &+\big((k+b)eX^*S^* + 2ebX^*S^*I^* + ebX^*(I^*)^2 + ekX^*I^* - (d_2 + mI^*)S^*\big) \end{aligned}$$

$$\boldsymbol{f^{(3)}(\varphi_3, \tilde{\varphi}_2, \tilde{\varphi}_3)} = -(d_2 + d_3)\varphi_3 + mI^*\tilde{\varphi}_2 + mS^*\tilde{\varphi}_3 + m\tilde{\varphi}_2\tilde{\varphi}_3 + mS^*I^*$$

$$f_{ilj}^{(1)} = \frac{\partial^{i+l+j} f^{(1)}}{\partial \varphi_1^i\, \varphi_2^l\, \varphi_3^j}\bigg|_{(\varphi_1,\varphi_2,\varphi_3)=(0,0,0)}$$

$$f_{ilj}^{(2)} = \frac{\partial^{i+l+j} f^{(2)}}{\partial \varphi_1^i\, \varphi_2^l\, \varphi_3^j}\bigg|_{(\varphi_1,\varphi_2,\varphi_3)=(0,0,0)}$$

$$f_{jkm}^{(3)} = \frac{\partial^{j+k+m} f^{(3)}}{\partial \varphi_3^j\, \tilde{\varphi}_2^k\, \tilde{\varphi}_3^m}\bigg|_{(\varphi_3,\tilde{\varphi}_2,\tilde{\varphi}_3)=(0,-1,-1)}$$

According the Riesz representation theorem [28], it can be find a 3×3 matrix function $\rho = (\vartheta, \eta)$ whose entries have bounded variation for $\vartheta \in [-1,0]$, such that

$$T_\eta(\varphi) = \int_{-1}^{0} d\,\rho(\vartheta, \eta)\, \varphi(\vartheta), \text{ for } \varphi \in C. \tag{33}$$

In reality, we can pick

$$\rho(\vartheta,\eta\,) = (\hat{\tau} + \eta)\big(A\delta(\vartheta) - B\delta(\vartheta+1)\big), \tag{34}$$

where $\delta(\vartheta)$ refers to the Dirac delta function.

For $\varphi \in C^1([-1,0],\mathbb{R}^3_+)$, define

$$A(\eta)\varphi(\vartheta) = \begin{cases} \frac{d\varphi(\vartheta)}{d\vartheta}, & -1 \le \vartheta < 0 \\ \int_{-1}^{0} d\,\rho(\vartheta,\eta\,)\,\varphi(\vartheta), & \vartheta = 0 \end{cases} \tag{35}$$

and

$$B(\eta)\varphi(\vartheta) = \begin{cases} 0, & -1 \le \vartheta < 0 \\ \mathrm{F}(\eta,\varphi), & \vartheta = 0 \end{cases}. \tag{36}$$

Then, system (1) becomes

$$\dot{W}(t) = A(\eta)W_t + B(\eta)W_t, \tag{37}$$

where $W_t(\vartheta) = W(t+\vartheta)$ for $\vartheta \in [-1,0]$.

For $\psi \in C^1([0,1],(\mathbb{R}^3_+)^*)$, define

$$A^*\psi(\kappa) = \begin{cases} -\frac{d\psi(\kappa)}{d\kappa}, & 0 < \kappa \le 1 \\ \int_{-1}^{0} d\,\rho^T(t,0\,)\,\psi(-t), & \kappa = 0 \end{cases} \tag{38}$$

and the bilinear inner product is offered below

$$\langle\psi(\kappa),\varphi(\vartheta)\rangle = \overline{\psi}(0)\,\varphi(0) - \int_{\vartheta=-1}^{0}\int_{\omega=0}^{\vartheta}\overline{\psi}(\omega-\vartheta)\;d\rho(\vartheta)\,\varphi(\omega)d\omega, \tag{39}$$

where $\rho(\vartheta) = \rho(\vartheta,0)$. Then $A = A(0)$ and A^* are adjoint operators. From the previous theorem (6), it is concluded that $\pm i\beta_0\hat{\tau}$ are eigenvalues of $A(0)$ and A^*, respectively. Using a simple computation, we can observe that

$$\left.\begin{aligned} q(\vartheta) &= (1,q_1,q_2)^T e^{i\beta_0\hat{\tau}\vartheta} \\ q^*(\kappa) &= D(1,q_1^*,q_2^*)^T e^{-i\beta_0\hat{\tau}\kappa} \end{aligned}\right\}, \tag{40}$$

where

$$q_1 = \frac{-\left(f_{100}^{(3)} + f_{100}^{(3)}\,e^{i\beta_0\hat{\tau}} - i\beta_0\right)q_2}{f_{010}^{(3)}\;e^{-i\beta_0\hat{\tau}}}$$

$$q_2 = \frac{-f_{100}^{(2)} f_{010}^{(3)} \ e^{-i\beta_0 \hat{\tau}}}{\beta_0^2 + f_{001}^{(2)} f_{001}^{(3)} \ e^{-i\beta_0 \hat{\tau}} + i\beta_0 \left(f_{010}^{(2)} + f_{100}^{(3)} + f_{100}^{(3)} \ e^{-i\beta_0 \hat{\tau}}\right) - f_{010}^{(2)} f_{100}^{(3)} \left(1 + e^{-i\beta_0 \hat{\tau}}\right)}$$

$$q_1^* = \frac{-\left(f_{100}^{(1)} + i\beta_0\right)}{f_{100}^{(2)}}$$

$$q_2^* = \frac{f_{100}^{(1)} f_{010}^{(2)} + i\beta_0 \left(f_{010}^{(2)} + f_{100}^{(1)}\right) - \left(\beta_0^2 + f_{010}^{(1)} f_{100}^{(2)}\right)}{f_{100}^{(2)} f_{010}^{(3)} \ e^{-i\beta_0 \hat{\tau}}}.$$

According to the normalization conditions $\langle q^*(\kappa), q(\vartheta)\rangle = 1$ and $\langle q^*(\kappa), \bar{q}(\vartheta)\rangle = 0$, it follows that

$$\begin{aligned} &\langle q^*(\kappa), q(\vartheta)\rangle = \bar{D}\left(1, \overline{q_1^*}, \overline{q_2^*}\right)(1, q_1, q_2)^T \\ &\int_{\vartheta=-1}^{0} \int_{\omega=0}^{\vartheta} \bar{D}\left(1, \overline{q_1^*}, \overline{q_2^*}\right) e^{-i(\omega-\vartheta)\beta_0 \hat{\tau}} \, d\rho(\vartheta) \, (1, q_1, q_2)^T \, e^{i\omega\beta_0 \hat{\tau}} d\omega \\ &= \bar{D}\left[1 + q_1 \, \overline{q_1^*} + q_2 \, \overline{q_2^*} + \overline{q_2^*}\left(q_1 f_{010}^{(3)} + q_2 f_{001}^{(3)}\right)\hat{\tau} e^{-i\beta_0 \hat{\tau}}\right] \end{aligned}$$

which provides

$$D = \frac{1}{1 + \overline{q_1} \, q_1^* + \overline{q_2} \, q_2^* + q_2^*\left(\overline{q_1} f_{010}^{(3)} + \overline{q_2} f_{001}^{(3)}\right)\hat{\tau} e^{i\beta_0 \hat{\tau}}}.$$

Next, applying a similar strategy as in [27], to compute the coefficients g_{ij} that determine the stability and direction of the Hopf bifurcation, it is obtained:

$$\begin{aligned} g(e, \bar{e}) &= \overline{q^*}(0) \, F_0(e, \bar{e}) \\ &= \hat{\tau} \bar{D}\left(1, \overline{q_1^*}, \overline{q_2^*}\right) \begin{pmatrix} U_1 \, e^2 + U_2 \, e\bar{e} + U_3 \, \bar{e}^2 + U_4 \, e^2\bar{e} + \cdots \\ U_5 \, e^2 + U_6 \, e\bar{e} + U_7 \, \bar{e}^2 + U_8 \, e^2\bar{e} + \cdots \\ U_9 \, e^2 + U_{10} \, e\bar{e} + U_{11} \, \bar{e}^2 + U_{12} \, e^2\bar{e} + \cdots \end{pmatrix} \\ &= P_1 \, e^2 + P_2 \, e\bar{e} + P_3 \, \bar{e}^2 + P_4 \, e^2\bar{e} + h.o.i. \end{aligned} \tag{41}$$

where $h.o.i.$ implies higher order items, and

$$P_1 = \hat{\tau} \, \bar{D}\left(U_1 + \overline{q_1^*} \, U_5 + \overline{q_2^*} \, U_9\right)$$

$$P_2 = \hat{\tau} \, \bar{D}\left(U_2 + \overline{q_1^*} \, U_6 + \overline{q_2^*} \, U_{10}\right)$$

$$P_3 = \hat{\tau} \, \bar{D}\left(U_3 + \overline{q_1^*} \, U_7 + \overline{q_2^*} \, U_{11}\right)$$

$$P_4 = \hat{\tau} \, \bar{D}\left(U_4 + \overline{q_1^*} \, U_8 + \overline{q_2^*} \, U_{12}\right)$$

with

$$U_1 = q_1 f_{110}^{(1)} + q_2 f_{101}^{(1)} + q_1 q_2 f_{011}^{(1)} + \frac{1}{2}\left(f_{200}^{(1)} + q_1^2 f_{020}^{(1)} + q_2^2 f_{002}^{(1)}\right)$$

$$U_2 = (q_1 + \overline{q_1})\, f_{110}^{(1)} + (q_2 + \overline{q_2})\, f_{101}^{(1)} + (q_1\, \overline{q_2} + q_2\, \overline{q_1})\, f_{011}^{(1)} + f_{200}^{(1)} + q_1\, \overline{q_1}\, f_{020}^{(1)} + q_2\, \overline{q_2}\, f_{002}^{(1)}$$

$$U_3 = \overline{q_1}\, f_{110}^{(1)} + \overline{q_2}\, f_{101}^{(1)} + \overline{q_1}\, \overline{q_2}\, f_{011}^{(1)} + \frac{1}{2}\left(f_{200}^{(1)} + \overline{q_1}^2\, f_{020}^{(1)} + \overline{q_2}^2\, f_{002}^{(1)}\right)$$

$$U_4 = \zeta_1\, f_{110}^{(1)} + \zeta_2\, f_{101}^{(1)} + \zeta_3\, f_{011}^{(1)} + \zeta_4\, f_{200}^{(1)} + \zeta_5\, f_{020}^{(1)} + \zeta_6\, f_{002}^{(1)}$$

$$U_5 = q_1\, f_{110}^{(2)} + q_2\, f_{101}^{(2)} + q_1 q_2\, f_{011}^{(2)} + \frac{1}{2}\left(q_1^2\, f_{020}^{(2)} + q_2^2\, f_{002}^{(2)}\right)$$

$$U_6 = (q_1 + \overline{q_1})\, f_{110}^{(2)} + (q_2 + \overline{q_2})\, f_{101}^{(2)} + (q_1\, \overline{q_2} + q_2\, \overline{q_1})\, f_{011}^{(2)} + q_1\, \overline{q_1}\, f_{020}^{(2)}$$

$$U_7 = \overline{q_1}\, f_{110}^{(2)} + \overline{q_2}\, f_{101}^{(2)} + \overline{q_1}\, \overline{q_2}\, f_{011}^{(2)} + \frac{1}{2}\left(\overline{q_1}^2\, f_{020}^{(2)} + \overline{q_2}^2\, f_{002}^{(2)}\right)$$

$$U_8 = \zeta_1\, f_{110}^{(2)} + \zeta_2\, f_{101}^{(2)} + \zeta_3\, f_{011}^{(2)} + \frac{1}{2}\left(\zeta_5\, f_{020}^{(2)} + \zeta_6\, f_{002}^{(2)}\right)$$

$$U_9 = q_1\, q_2\, f_{011}^{(3)}\, e^{-2i\beta_0\tau\hat{}}$$

$$U_{10} = (q_1\, \overline{q_2} + q_2\, \overline{q_1})\, f_{011}^{(3)}$$

$$U_{11} = \overline{q_1}\, \overline{q_2}\, f_{011}^{(3)}\, e^{2i\beta_0\tau\hat{}}$$

$$U_{12} = \zeta_7\, f_{011}^{(3)}$$

here

$$\zeta_1 = q_1\, W_{11}^{(1)}(0) + W_{11}^{(2)}(0) + \frac{1}{2}\, \overline{q_1}\, W_{20}^{(1)}(0) + \frac{1}{2}\, W_{20}^{(2)}(0)$$

$$\zeta_2 = q_2\, W_{11}^{(1)}(0) + W_{11}^{(3)}(0) + \frac{1}{2}\, \overline{q_2}\, W_{20}^{(1)}(0) + \frac{1}{2}\, W_{20}^{(3)}(0)$$

$$\zeta_3 = q_2\, W_{11}^{(2)}(0) + W_{11}^{(3)}(0) + \frac{1}{2}\, \overline{q_2}\, W_{20}^{(2)}(0) + \frac{1}{2}\, \overline{q_1}\; W_{20}^{(3)}(0)$$

$$\zeta_4 = W_{11}^{(1)}(0) + \frac{1}{2}\, W_{20}^{(1)}(0)$$

$$\zeta_5 = q_1\, W_{11}^{(2)}(0) + \frac{1}{2}\, \overline{q_1}\, W_{20}^{(2)}(0)$$

$$\zeta_6 = q_2\, W_{11}^{(3)}(0) + \frac{1}{2}\, \overline{q_2}\, W_{20}^{(3)}(0)$$

$$\zeta_7 = \left(q_2\, W_{11}^{(2)}(-1) + q_1\, W_{11}^{(3)}(-1)\right) e^{-i\beta_0\tau\hat{}} + \frac{1}{2}\left(\overline{q_2}\, W_{20}^{(2)}(-1) + \overline{q_1}\, W_{20}^{(3)}(-1)\right) e^{i\beta_0\tau\hat{}}$$

Simplifying the equation (41), it yields

$$g_{20} = 2P_1, g_{11} = P_2, g_{02} = 2P_3, g_{21} = 2P_4. \tag{42}$$

Clearly, in order to complete the computation of the coefficients g_{ij} in equation (42), it is necessary to compute:

$$W_{20}(\vartheta) = \left(W_{20}^{(1)}(\vartheta), W_{20}^{(2)}(\vartheta), W_{20}^{(3)}(\vartheta)\right)^T,\ W_{11}(\vartheta) = \left(W_{11}^{(1)}(\vartheta), W_{11}^{(2)}(\vartheta), W_{11}^{(3)}(\vartheta)\right)^T.$$

A straightforward calculation yields

$$\left.\begin{aligned} W_{20}(\vartheta) &= \frac{ig_{20}}{\beta_0\hat{\tau}}\ q(0)\, e^{i\beta_0\hat{\tau}\vartheta} + \frac{i\bar{g}_{20}}{3\,\beta_0\hat{\tau}}\ \bar{q}(0)\, e^{-i\beta_0\hat{\tau}\vartheta} + R_1\, e^{2i\beta_0\hat{\tau}\vartheta} \\ W_{11}(\vartheta) &= -\frac{ig_{11}}{\beta_0\hat{\tau}}\ q(0)\, e^{i\beta_0\hat{\tau}\vartheta} + \frac{i\bar{g}_{11}}{\beta_0\hat{\tau}}\ \bar{q}(0)\, e^{-i\beta_0\hat{\tau}\vartheta} + R_2 \end{aligned}\right\} \tag{43}$$

where $R_1 = \left(R_1^{(1)}, R_1^{(2)}, R_1^{(3)}\right)^T$, and $R_2 = \left(R_2^{(1)}, R_2^{(2)}, R_2^{(3)}\right)^T \in \mathbb{R}^3$ are constant vectors that satisfy the following equations:

$$\begin{pmatrix} 2i\beta_0 - f_{100}^{(1)} & -f_{010}^{(1)} & -f_{001}^{(1)} \\ -f_{100}^{(2)} & 2i\beta_0 - f_{010}^{(2)} & -f_{001}^{(2)} \\ 0 & -f_{010}^{(3)}\, e^{2i\beta_0\hat{\tau}\vartheta} & 2i\beta_0 - f_{100}^{(3)}\, e^{2i\beta_0\hat{\tau}\vartheta} \end{pmatrix} R_1 = 2\begin{pmatrix} U_1 \\ U_5 \\ U_9 \end{pmatrix} \tag{44}$$

$$\begin{pmatrix} -f_{100}^{(1)} & -f_{010}^{(1)} & -f_{001}^{(1)} \\ -f_{100}^{(2)} & -f_{010}^{(2)} & -f_{001}^{(2)} \\ 0 & -f_{010}^{(3)} & -f_{100}^{(3)} \end{pmatrix} R_2 = \begin{pmatrix} U_2 \\ U_6 \\ U_{10} \end{pmatrix} \tag{45}$$

Using Cramer's rule, it is obtained that:

$$R_1^{(i)} = \frac{|\mathcal{H}_{1i}|}{|\mathcal{H}_1|}\ \text{, and}\quad R_2^{(i)} = \frac{|\mathcal{H}_{2i}|}{|\mathcal{H}_2|}\quad \text{for}\ \ i = 1, 2, 3, \tag{46}$$

Where

$$\mathcal{H}_1 = \begin{pmatrix} 2i\beta_0 - f_{100}^{(1)} & -f_{010}^{(1)} & -f_{001}^{(1)} \\ -f_{100}^{(2)} & 2i\beta_0 - f_{010}^{(2)} & -f_{001}^{(2)} \\ 0 & -f_{010}^{(3)}\, e^{2i\beta_0\hat{\tau}\vartheta} & 2i\beta_0 - f_{100}^{(3)}\, e^{2i\beta_0\hat{\tau}\vartheta} \end{pmatrix}.$$

$$\mathcal{H}_2 = \begin{pmatrix} -f_{100}^{(1)} & -f_{010}^{(1)} & -f_{001}^{(1)} \\ -f_{100}^{(2)} & -f_{010}^{(2)} & -f_{001}^{(2)} \\ 0 & -f_{010}^{(3)} & -f_{100}^{(3)} \end{pmatrix}.$$

$$\mathcal{H}_{11} = \begin{pmatrix} U_1 & -f_{010}^{(1)} & -f_{001}^{(1)} \\ U_5 & 2i\beta_0 - f_{010}^{(2)} & -f_{001}^{(2)} \\ U_9 & -f_{010}^{(3)}\, e^{2i\beta_0\hat{\tau}\vartheta} & 2i\beta_0 - f_{100}^{(3)}\, e^{2i\beta_0\hat{\tau}\vartheta} \end{pmatrix}.$$

$$\mathcal{H}_{12}=\begin{pmatrix} 2i\beta_0-f_{100}^{(1)} & U_1 & -f_{001}^{(1)} \\ -f_{100}^{(2)} & U_5 & -f_{001}^{(2)} \\ 0 & U_9 & 2i\beta_0-f_{100}^{(3)}\,e^{2i\beta_0\tau\hat{}\,\vartheta} \end{pmatrix}.$$

$$\mathcal{H}_{13}=\begin{pmatrix} 2i\beta_0-f_{100}^{(1)} & -f_{010}^{(1)} & U_1 \\ -f_{100}^{(2)} & 2i\beta_0-f_{010}^{(2)} & U_5 \\ 0 & -f_{010}^{(3)}\,e^{2i\beta_0\tau\hat{}\,\vartheta} & U_9 \end{pmatrix}.$$

$$\mathcal{H}_{21}=\begin{pmatrix} U_2 & -f_{010}^{(1)} & -f_{001}^{(1)} \\ U_6 & -f_{010}^{(2)} & -f_{001}^{(2)} \\ U_{10} & -f_{010}^{(3)} & -f_{100}^{(3)} \end{pmatrix}.$$

$$\mathcal{H}_{22}=\begin{pmatrix} -f_{100}^{(1)} & U_2 & -f_{001}^{(1)} \\ -f_{100}^{(2)} & U_6 & -f_{001}^{(2)} \\ 0 & U_{10} & -f_{100}^{(3)} \end{pmatrix}.$$

$$\mathcal{H}_{23}=\begin{pmatrix} -f_{100}^{(1)} & -f_{010}^{(1)} & U_2 \\ -f_{100}^{(2)} & -f_{010}^{(2)} & U_6 \\ 0 & -f_{010}^{(3)} & U_{10} \end{pmatrix}.$$

Therefore, according to equation (43) the values of $W_{20}(\vartheta)$ and $W_{11}(\vartheta)$ can be estimated. As a result, determining the coefficients g_{ij} become possible. Finally, the following biological expressions will be generated based on the values of g_{ij}.

$$\left.\begin{aligned} C_1(0)&=\frac{i}{2\beta_0\tau\hat{}}\left(g_{11}\;g_{20}-2|g_{11}|^2-\frac{1}{3}\;|g_{02}|^2\right)+\frac{1}{2}\;g_{21} \\ \mathcal{M}_2&=-\frac{Re\{C_1(0)\}}{Re\{\lambda'(\tau\hat{})\}} \\ \Upsilon_2&=2Re\{C_1(0)\} \\ \mathrm{T}_2&=-\frac{Im\{C_1(0)\}+\mathcal{M}_2\,Im\left\{Re\{\lambda'(\tau\hat{})\}\right\}}{\beta_0\tau\hat{}} \end{aligned}\right\} \tag{47}$$

Furthermore, the following theorem will be used to explore the dynamical features of cyclic solutions caused at $\tau=\tau\hat{}$ using the preceding formulas [14].

Theorem 7. The following outcomes are achieved for the system (1) at $\tau=\tau\hat{}$.

i. Direction of the Hopf bifurcation is forward (backward) if $\mathcal{M}_2>0$ ($\mathcal{M}_2<0$), the cyclic solutions exist for $\tau>\tau\hat{}(\tau<\tau\hat{})$.
ii. The bifurcating cyclic solutions on the center manifold are stable (unstable) if $\Upsilon_2<0$ ($\Upsilon_2>0$).

iii. Period of the bifurcating cyclic solutions increases (decreases) if $T_2 > 0$ ($T_2 < 0$).

8. NUMERICAL SIMULATION

The key results are numerically shown in this section using the biologically plausible hypothetical set of values listed below. The goal is to validate the theoretically generated results and understand the parameters' influence on the system dynamics (1).

$$r = 1, a = 0.1, d_1 = 0.05, c = 0.3, k = 0.5, b = 0.1, e = 0.5$$
$$d_2 = 0.1, m = 0.3, d_3 = 0.1, \tau = 0.5. \quad (48)$$

It is noted that, the solution of system (1) approaches E_0, E_1, E_2, E^*, and 3D periodic attractor for the ranges $(0,0.05]$, $(0.05,0.2)$, $[0.2,0.6)$, $[0.6,2.7)$, and $r \geq 2.7$ respectively, as explained in the Figure (2) below at a selected values of r.

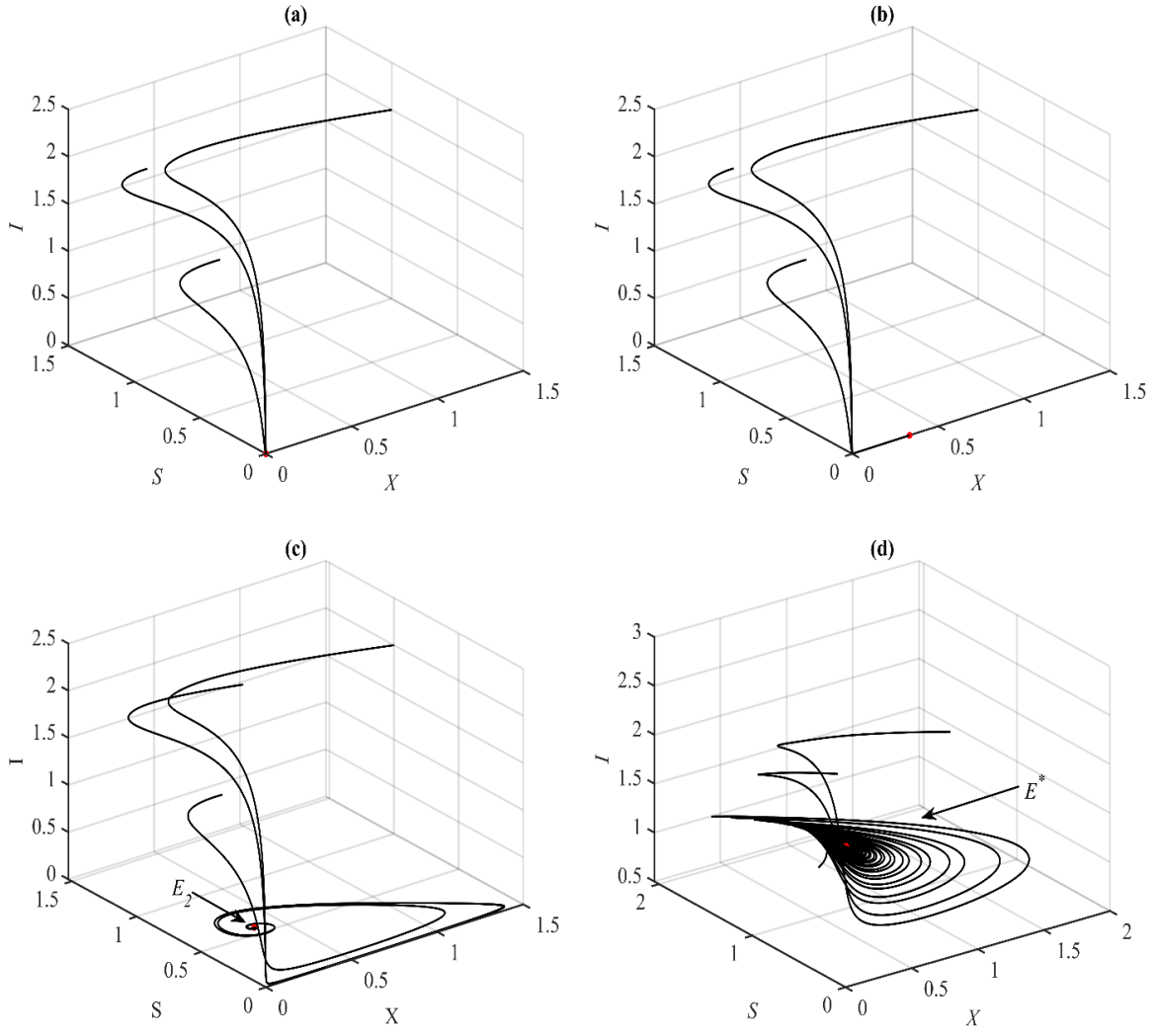

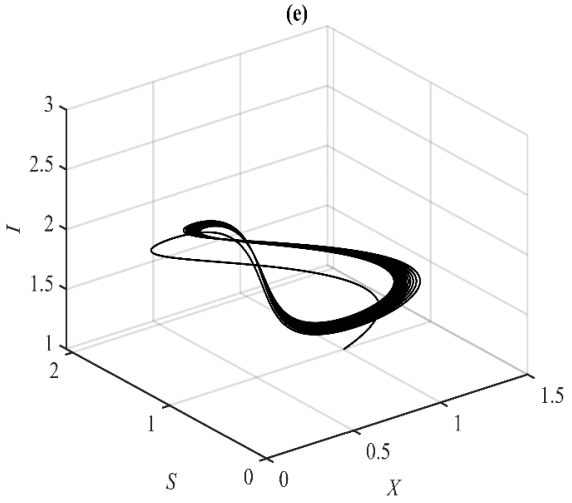

Fig. 2: The phase portraits of system (1) utilizing data set (48) and starting from different initial points with different values of r. **(a)** Approaches to E_0 when $r = 0.05$. **(b)** Approaches to $E_1 = (0.33,0,0)$ when $r = 0.15$. **(c)** Approaches to $E_2 = (0.35,0.56,0)$ when $r = 0.5$. **(d)** Approaches to $E^* = (0.47,0.66,1.4)$ when $r = 2$. **(e)** Approaches to 3D periodic attractor when $r = 3$.

Figure (2) shows that system (1) has four bifurcation points falling in the r range, confirming the theoretical results.

The influence of varying the parameter a on the dynamics of system (1) is explained in Figures (3) and (4) below.

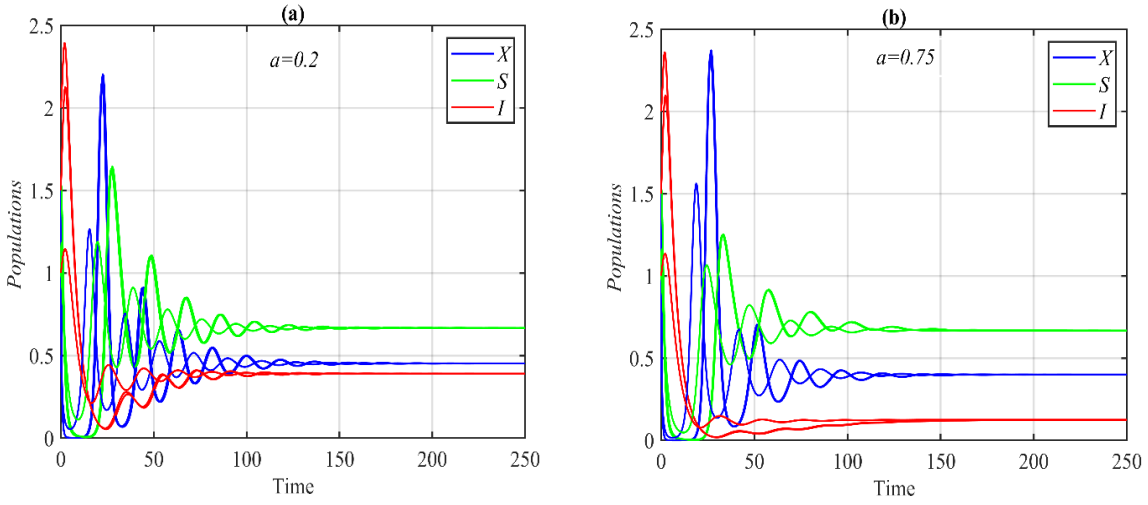

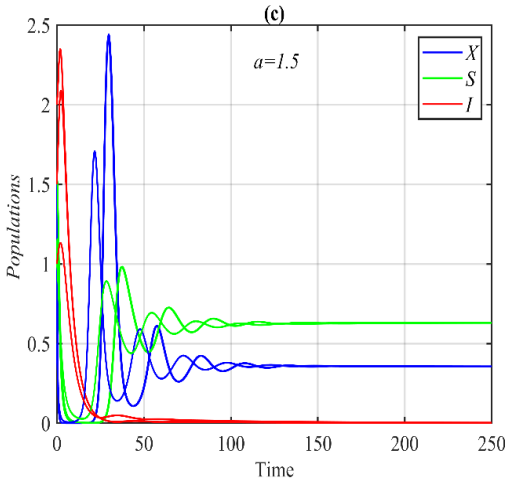

Fig. 3: The time series of the system (1) utilizing data set (48) and starting from different initial points with different values of a. **(a)** Approaches to $E^* = (0.45,0.66,0.38)$ when $a = 0.2$. **(b)** Approaches to $E^* = (0.39,0.66,0.12)$ when $a = 75$. **(c)** Approaches to$E_2 = (0.35,0.63,0)$ when $a = 1.5$.

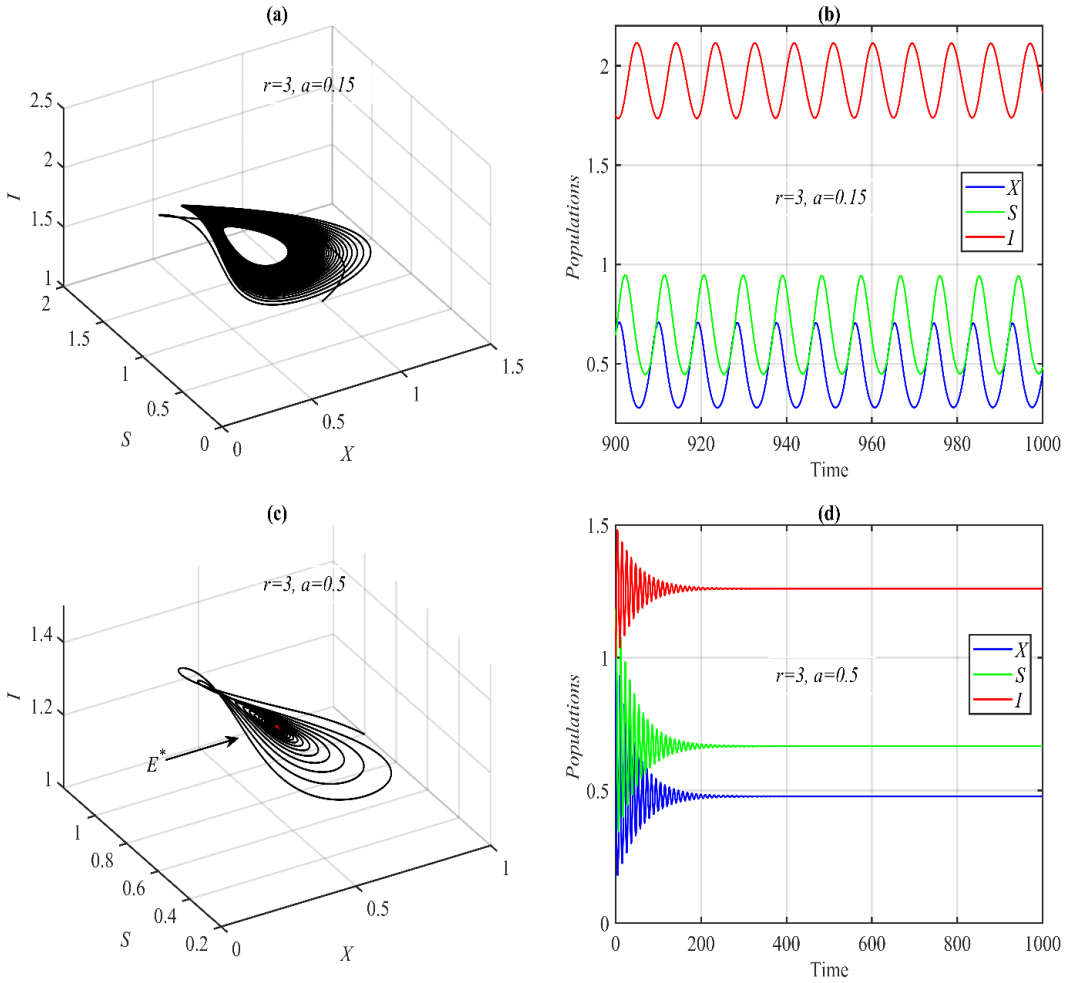

Fig. 4: The phase portraits and their time series of the system (1) utilizing data set (48) with different values of a and $r = 3$. **(a)** Approaches to 3D periodic attractor when $a = 0.15$. **(b)** Time series when $a = 0.15$ and $r = 3$. **(c)** Approaches to $E^* = (0.47,0.66,1.26)$ when $a = 0.5$ and $r = 3$. **(d)** Time series when $a = 0.5$ and $r = 3$.

Clearly, Figures (3) and (4) show that increasing the value of a transfers the periodic dynamics to a stable case at E^*. However, increasing this value further transfers the stability from E^* to E_2.

Now, Figure (5) studied the influence of varying the parameter d_1 with the rest of parameters values as in (48).

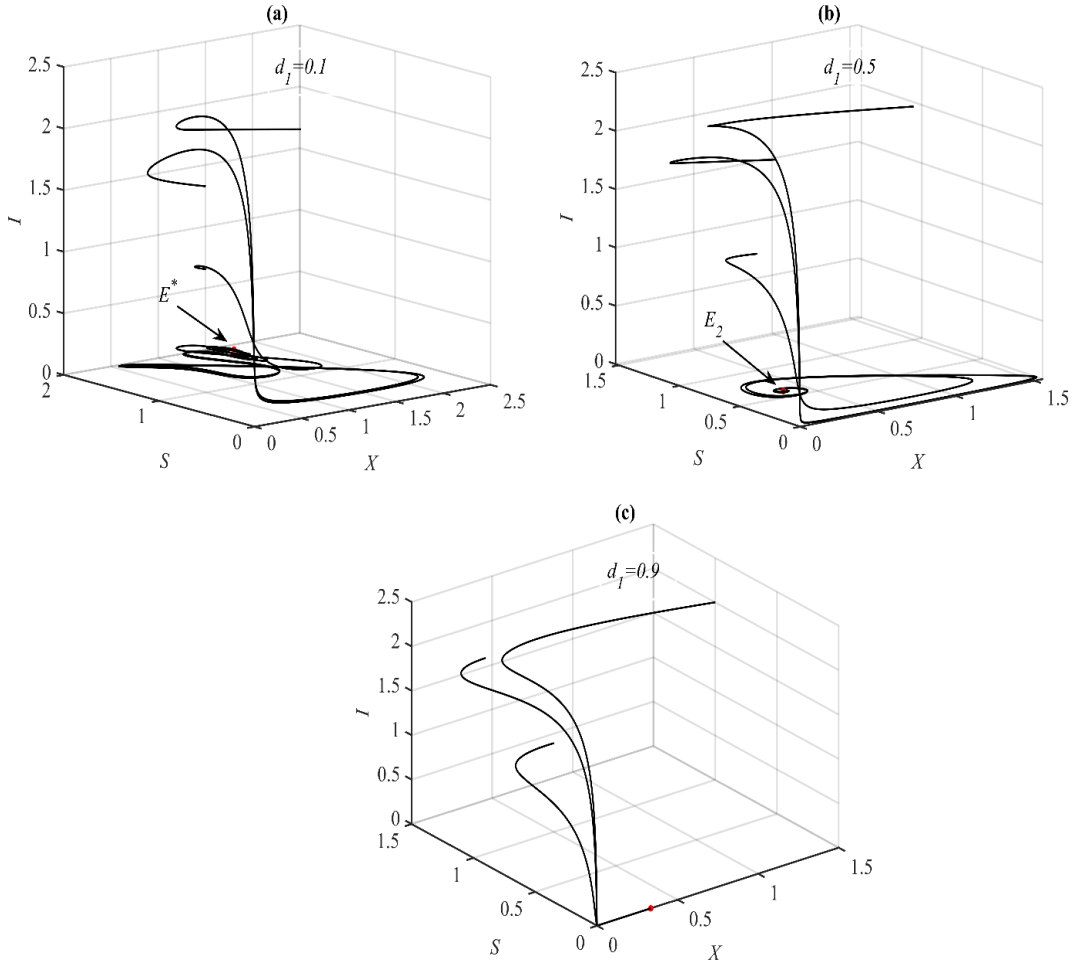

Fig. 5: The phase portraits of system (1) utilizing data set (48) and starting from different initial points with different values of d_1. **(a)** Approaches to $E^* = (0.45,0.66,0.42)$ when $d_1 = 0.1$. **(b)** Approaches to $E_2 = (0.35,0.6,0)$ when $d_1 = 0.5$. **(c)** Approaches to $E_1 = (0.33,0,0)$ when $d_1 = 0.9$.

It is obtained that for the ranges $(0,0.45)$, $[0.45,0.88)$, and $[0.88,1]$ the solution of system (1) goes asymptotically to E^*, E_2, and E_1 respectively as in Figure (5a), (5b), and (5c) at selected values.

The impact of varying the parameter c is investigated in Figure (6). It is noted that, the solution of system (1) approaches asymptotically to 3D periodic attractor, E^*, E_2, and E_1 for the rangers $(0,0.14]$, $(0.4,1.5)$, $[1.5,2.4)$, and $c \geq 2.4$ respectively.

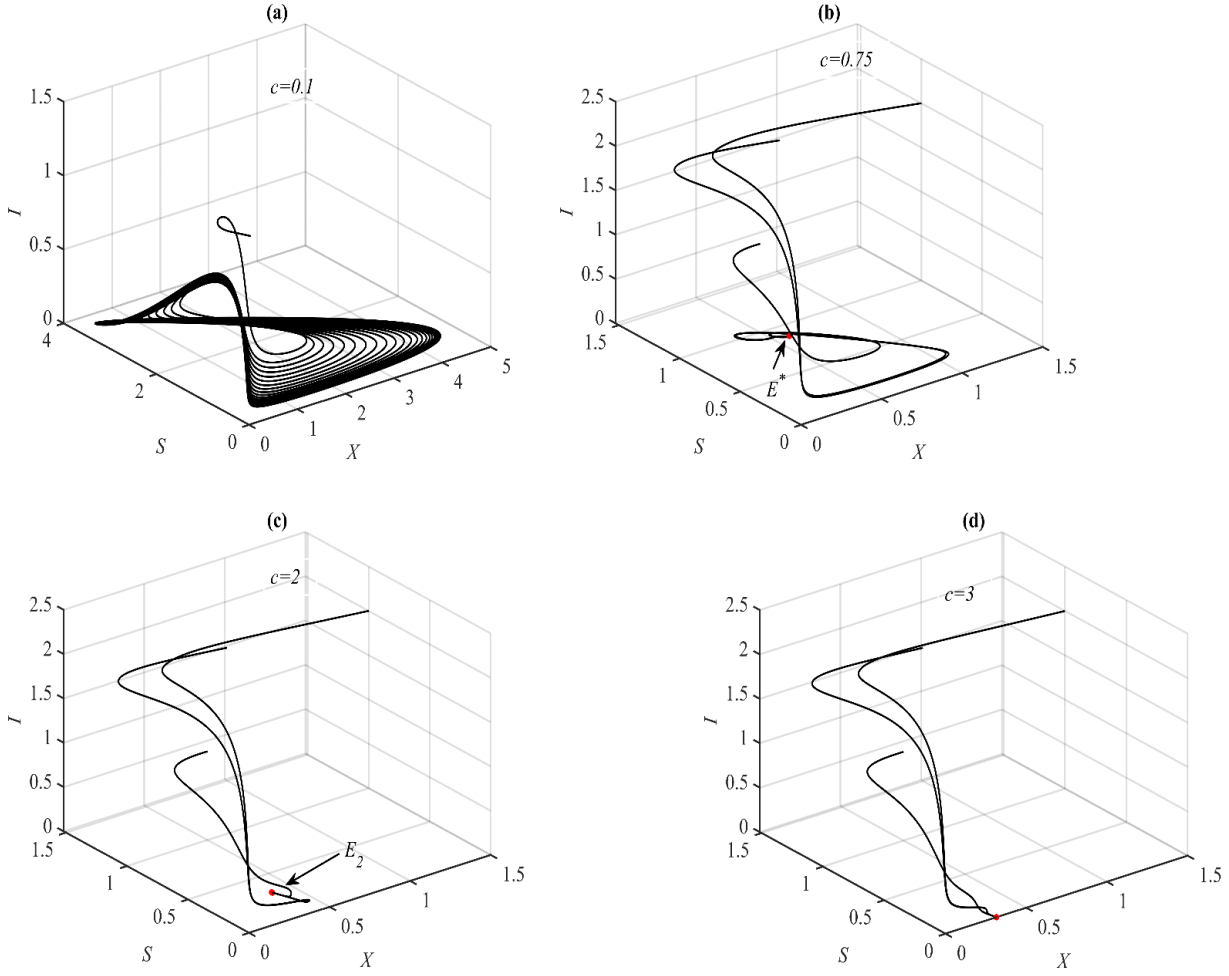

Fig. 6: The phase portraits of system (1) utilizing data set (48) and starting from different initial points with different values of c. **(a)** Approaches to 3D periodic attractor when $c = 0.1$. **(b)** Approaches to $E^* = (0.43,0.66,0.25)$ when $c = 0.75$. **(c)** Approaches to $E_2 = (0.37,0.31,0)$ when $c = 2$. **(d)** Approaches to $E_1 = (0.31,0,0)$ when $c = 3$.

Accordingly, system (1) has three bifurcation points falling in the c range. Moreover, the impacts of varying k and b on the system (1) dynamics are studied numerically and the obtained results for the some selected values of them are shown in Figure (7) and (8) respectively.

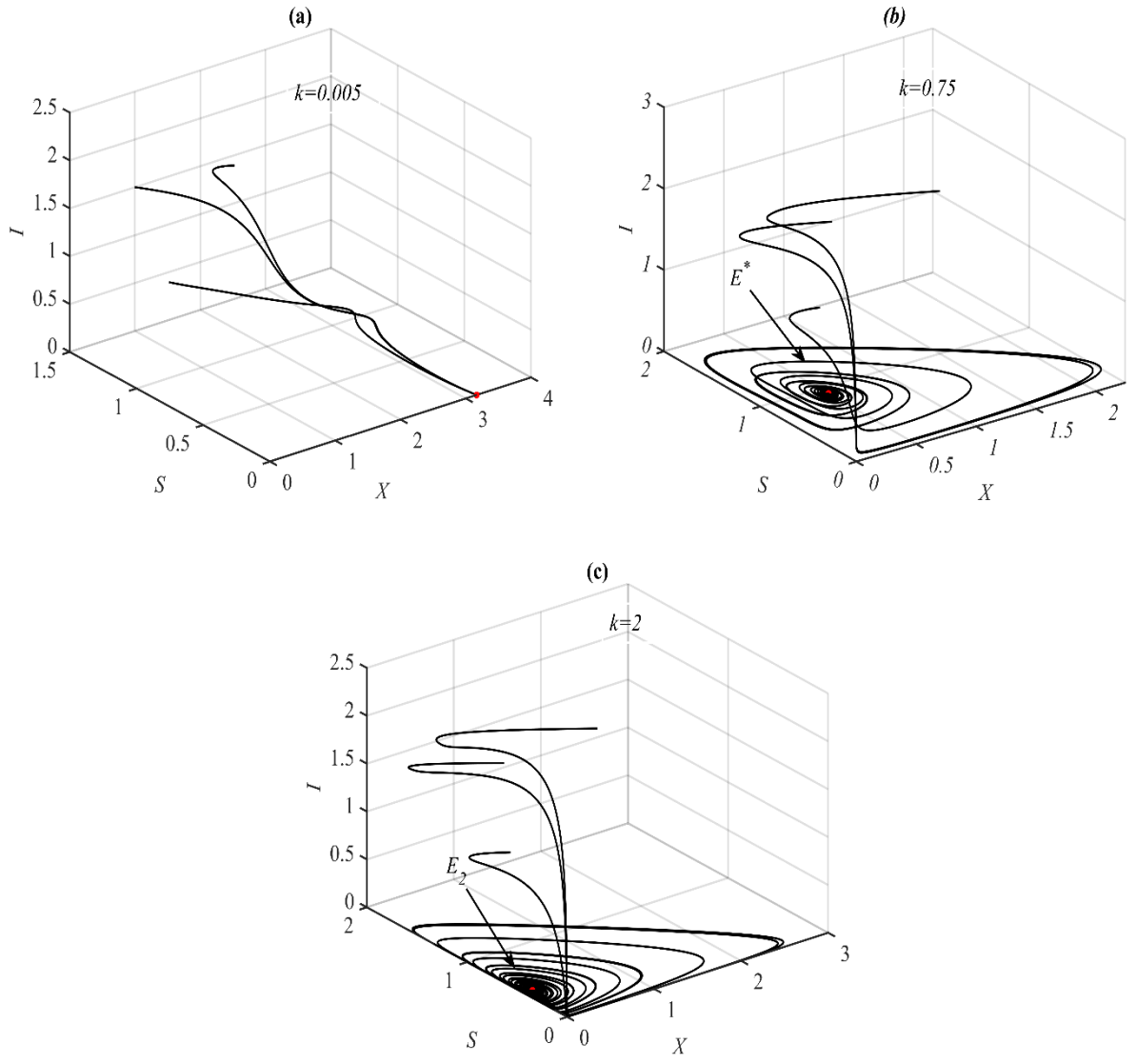

Fig. 7: The phase portraits of the system (1) utilizing data set (48) and starting from different initial points with different values of k. **(a)** Approaches to $E_1 = (3.16,0,0)$ when $k = 0.005$. **(b)** Approaches to $E^* = (0.3,0.66,0.25)$ when $k = 0.75$. **(c)** Approaches to $E_2 = (0.09,0.43,0)$ when $k = 2$.

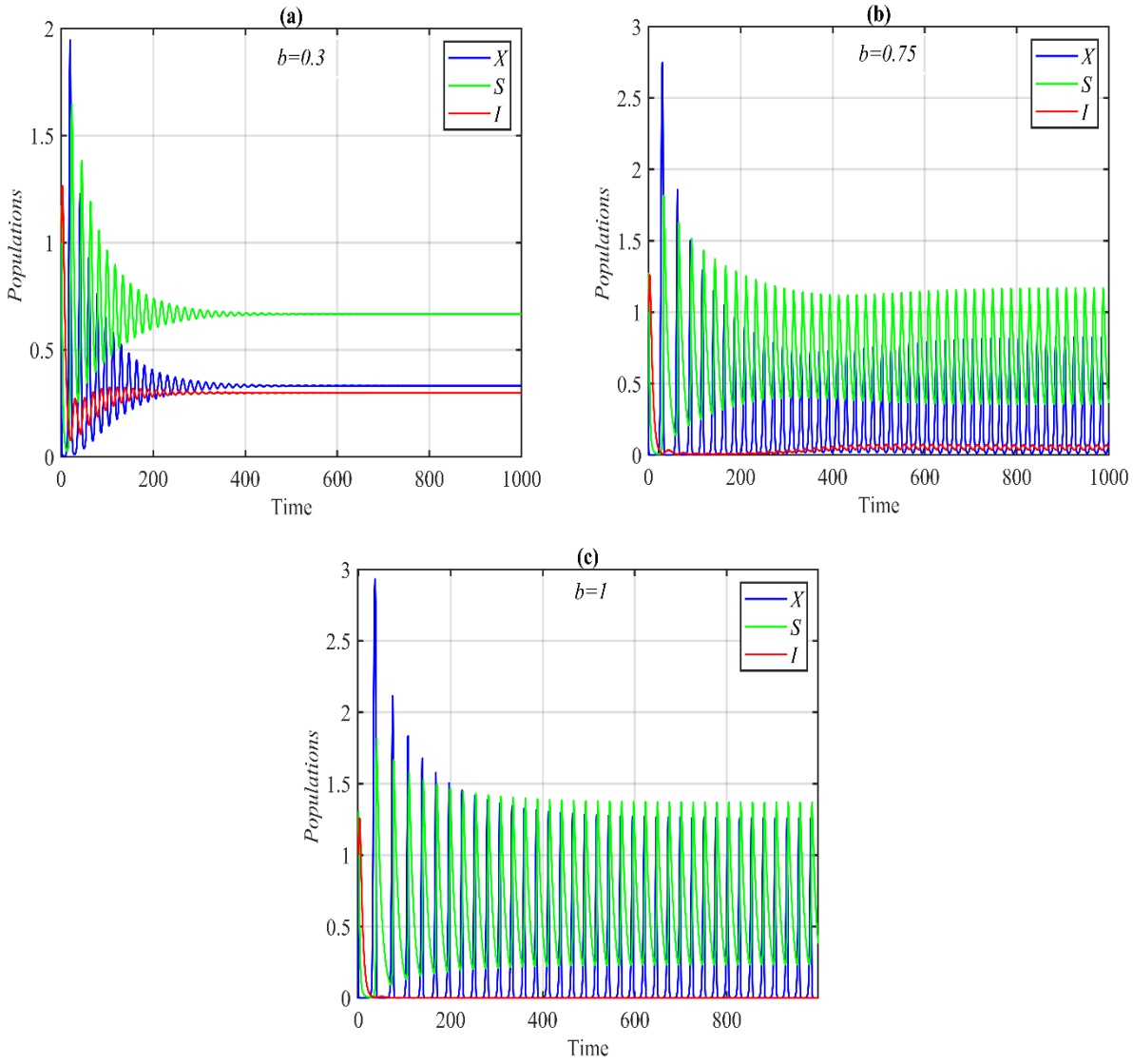

Fig. 8: The time series of system (1) utilizing data set (48) with different values of b. **(a)** Approaches to $E^* = (0.33,0.66,0.29)$ when $b = 0.3$. **(b)** Approaches to 3D periodic attractor when $b = 0.75$. **(c)** Approaches to 2D periodic attractor when $b = 1$.

It is observed that for the k ranges $(0,0.005]$, $(0.005,1.2)$, and $k \geq 1.2$ the solution of system (1) approaches E_1, E^*, and E_2 respectively. However, it approaches E^*, 3D periodic attractor, and 2D periodic attractor when $b \in (0,0.5)$, $b \in [0.5,0.9)$, and $b \geq 0.9$.

The behavior of system (1) dynamics as a function of the parameter e is studied numerically and the obtained results are explained in Figure (9) at some selected values.

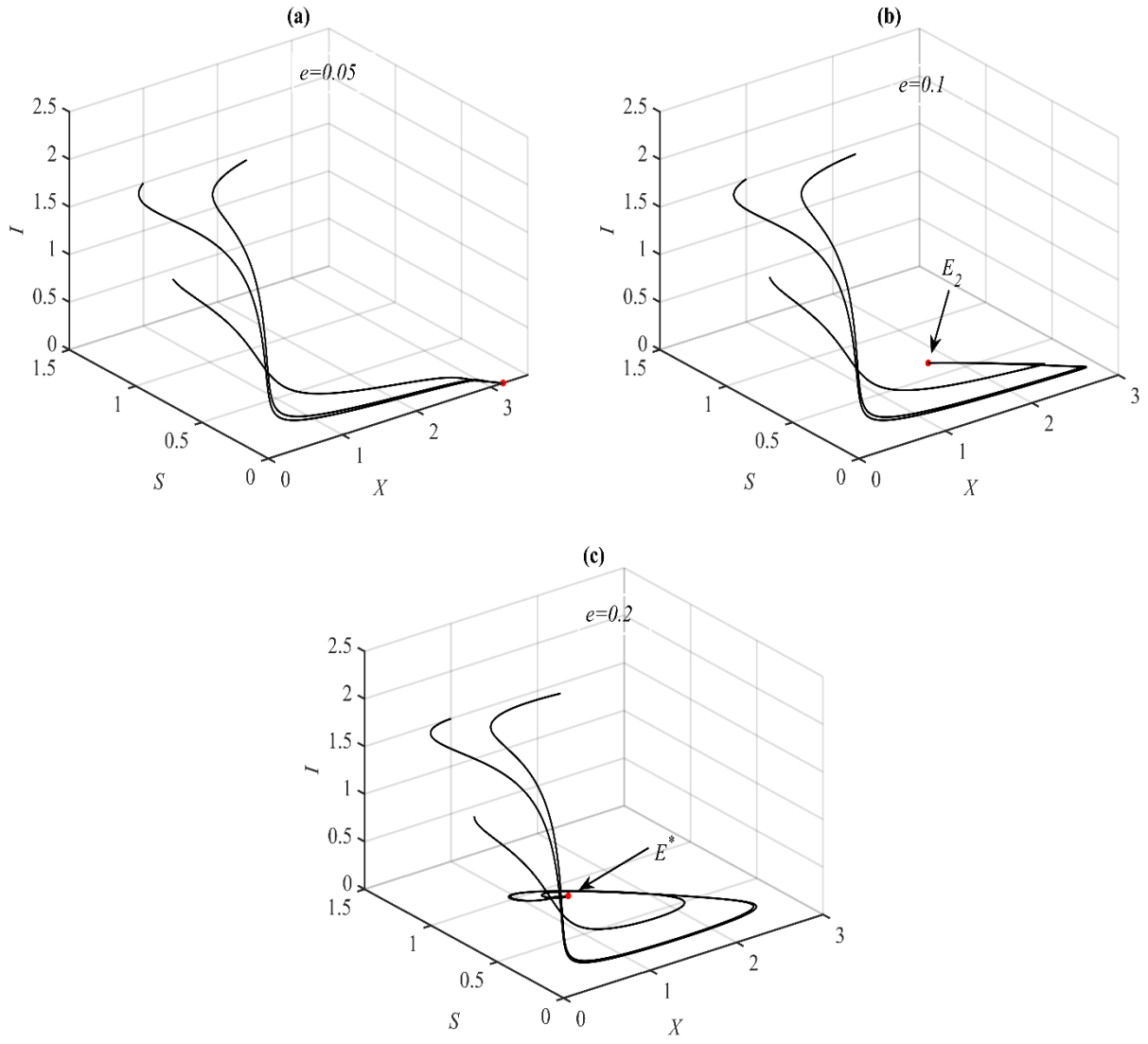

Fig. 9: The phase portraits of system (1) utilizing data set (48) and starting from different initial points with different values of e. **(a)** Approaches to $E_1 = (3.16,0,0)$ when $e = 0.05$. **(b)** Approaches to $E_2 = (1.77,0.63,0)$ when $e = 0.1$. **(c)** Approaches to $E^* = (1.07,0.66,0.25)$ when $e = 0.2$.

It is observed that for the e ranges $(0,0.066)$, $[0.07,0.12)$, and $[0.12,1]$ the solution of system (1) approaches E_1, E_2, and E^* respectively. However, the impact of varying the parameters d_2, m, and d_3 on the system (1) dynamics are studied numerically and the obtained results at some selected values are explained in Figures (10), (11), and (12).

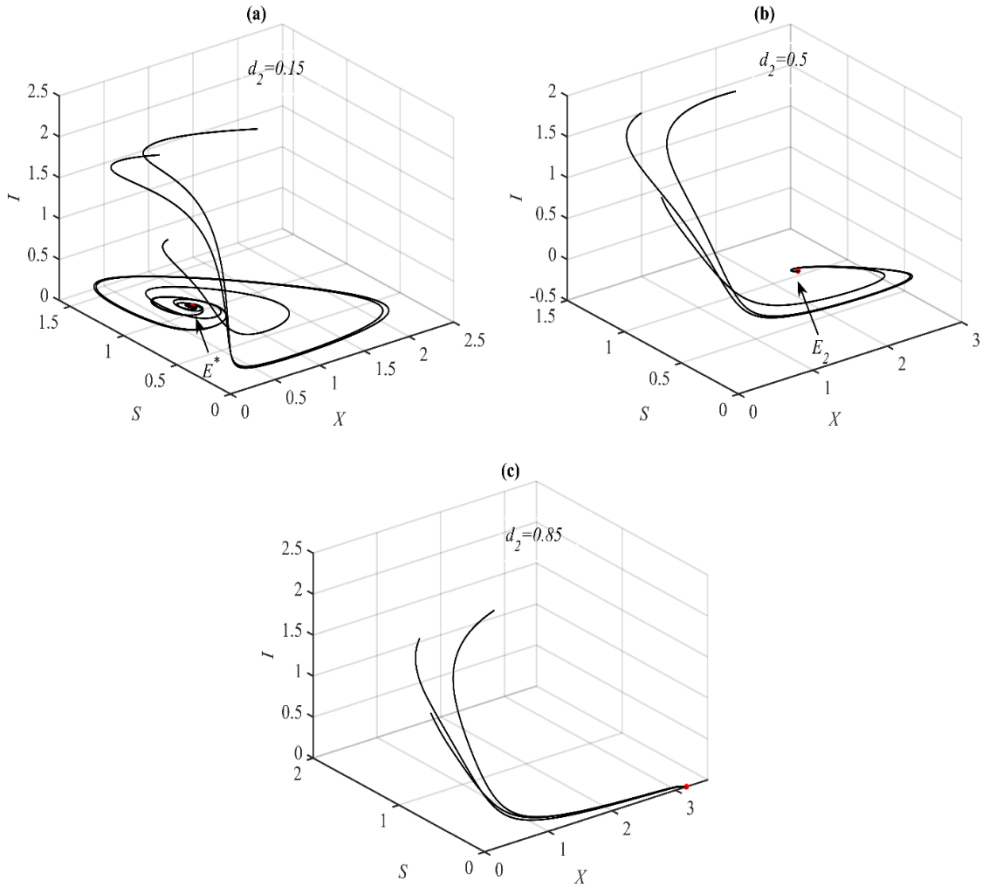

Fig. 10: The phase portraits of system (1) utilizing data set (48) and starting from different initial points with different values of d_2. **(a)** Approaches to $E^* = (0.57,0.83,0.27)$ when $d_2 = 0.15$. **(b)** Approaches to $E_2 = (1.77,0.63,0)$ when $d_2 = 0.5$. **(c)** Approaches to $E_1 = (3.16,0,0)$ when $d_2 = 0.85$.

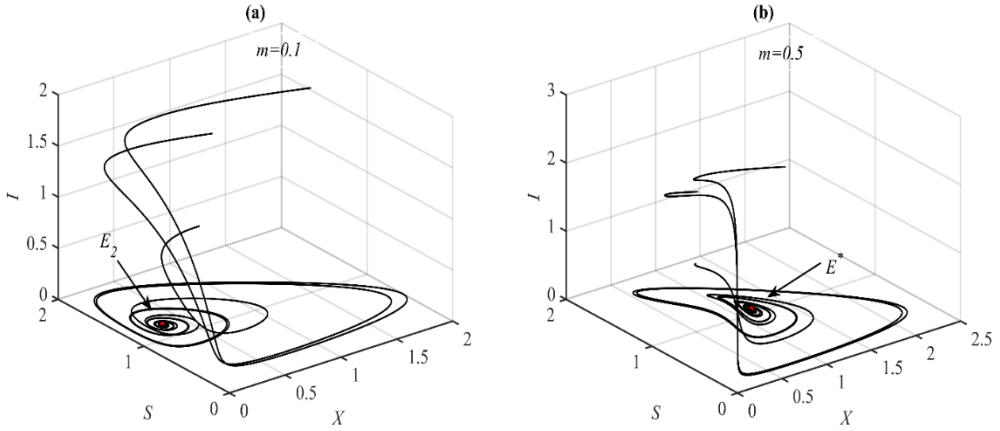

Fig. 11: The phase portraits of system (1) utilizing data set (48) and starting from different initial points with different values of m. **(a)** Approaches to $E_2 = (0.32,1.2,0)$ when $m = 0.1$. **(b)** Approaches to $E^* = (0.53,0.4,0.72)$ when $m = 0.5$.

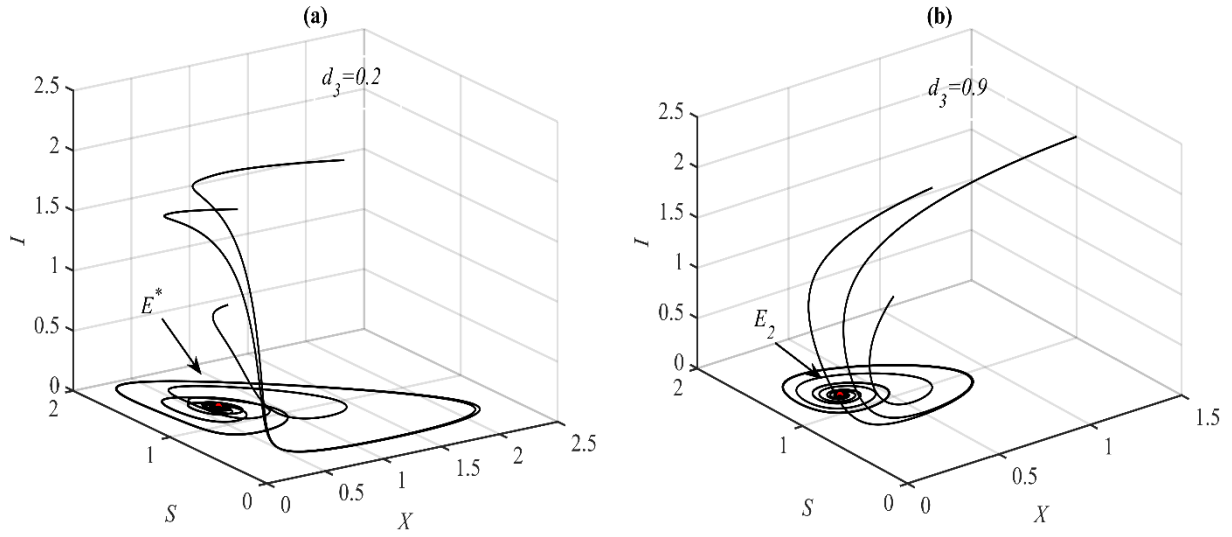

Fig. 12: The phase portraits of system (1) utilizing data set (48) and starting from different initial points with different values of d_3. **(a)** Approaches to $E^* = (0.41,1,0.16)$ when $d_3 = 0.2$. **(b)** Approaches to $E_2 = (0.32,1.2,0)$ when $d_3 = 0.9$.

It is noted that, for the d_2 ranges $(0,0.22)$, $[0.22,0.79)$, and $[0.79,1]$ the system (1) solution approaches E^*, E_2, and E_1 respectively. For the m ranges $(0,0.17)$, and $m \geq 0.17$ the system (1) solution approaches E_2, and E^* respectively. However, for the d_3 ranges $(0,0.26)$, and $[0.26,1]$ the system (1) solution approaches E^* and E_2 respectively.

On the other hand, the influence of delay on the system (1) dynamics is investigated numerically using the following set of data.

$$r = 2, a = 0.1, d_1 = 0.05, c = 0.3, k = 0.5, b = 0.2, e = 0.5$$
$$d_2 = 0.1, m = 0.3, d_3 = 0.1, \tau = 2. \quad (49)$$

It is obtained that, for the data set (49), the solution approaches asymptotically to E^*, while as the parameter τ exceeds the value $\hat{\tau} \cong 9.4$ the system (1) undergoes a Hopf bifurcation and the size of bifurcating periodic linearly proportional with value of τ before it returns to stable at E^* and so on, see Figure (13) for selected values of τ.

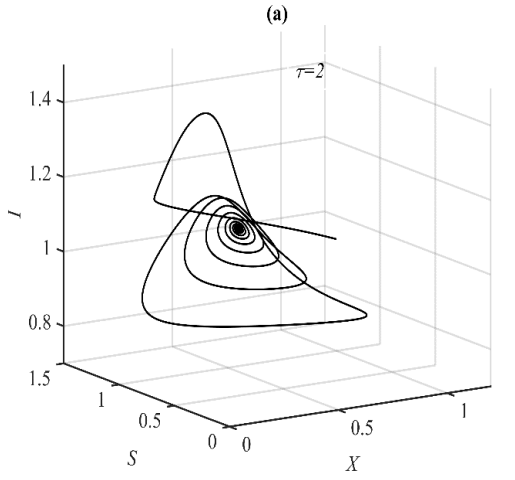
(a)
τ=2
I
S
X

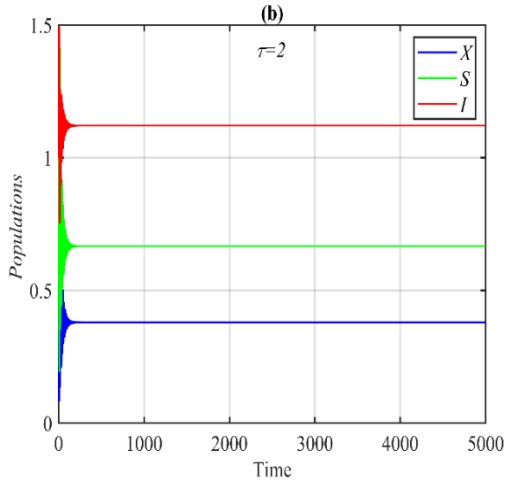
(b)
τ=2
X
S
I
Populations
Time

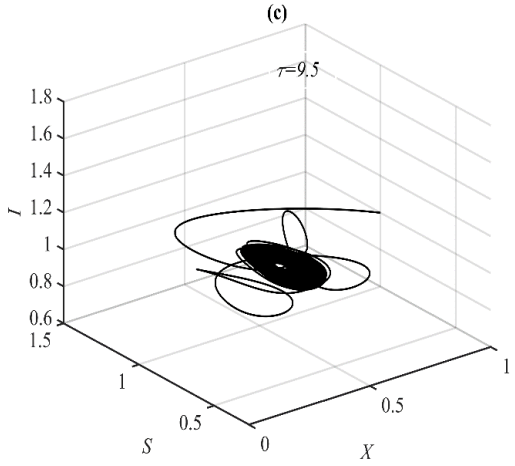
(c)
τ=9.5
I
S
X

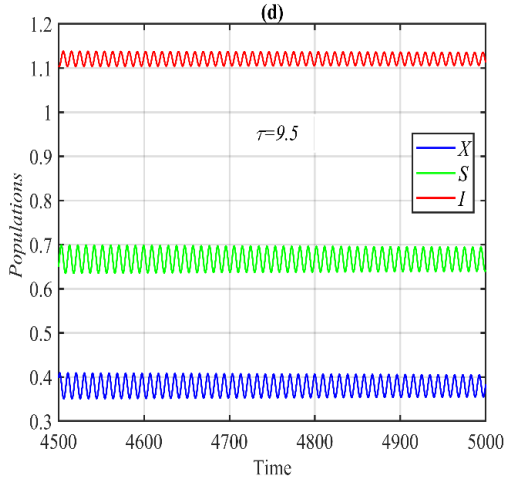
(d)
τ=9.5
X
S
I
Populations
Time

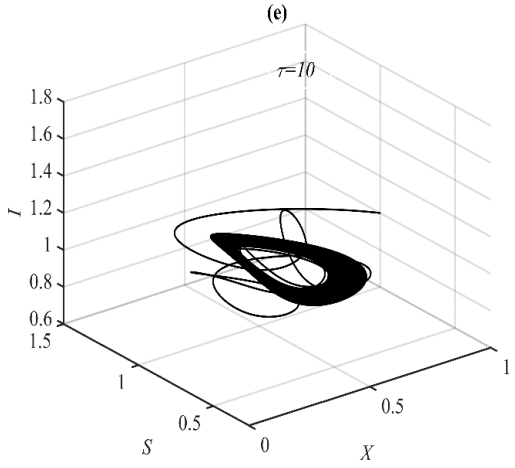
(e)
τ=10
I
S
X

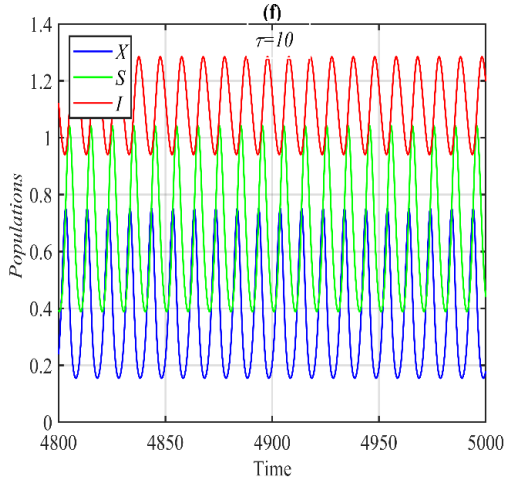
(f)
τ=10
X
S
I
Populations
Time

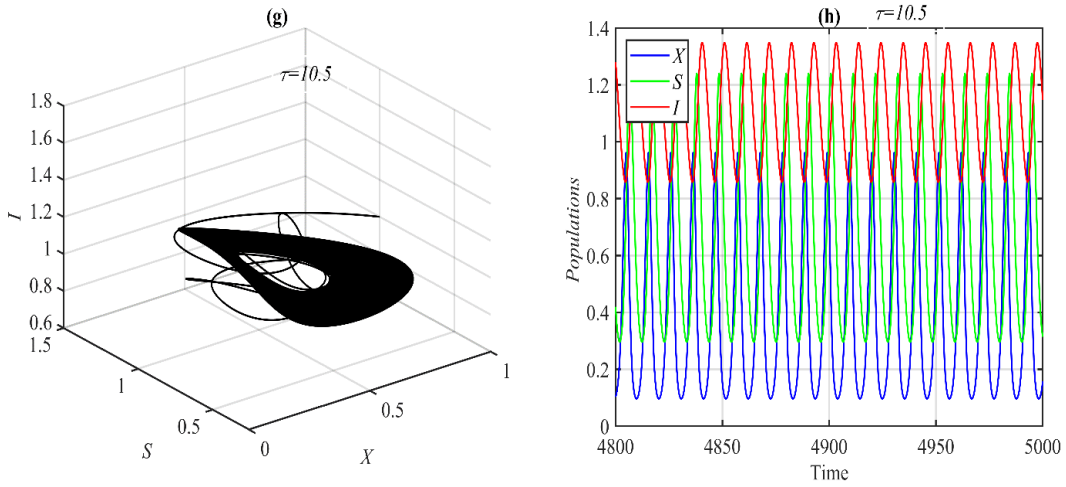

Fig. 13: The phase portraits and their time series of system (1) utilizing data set (49) with different values of τ. **(a)** Approaches to $E^* = (0.37,0.66,1.12)$ when $\tau = 2$. **(b)** Time series when $\tau = 2$. **(c)** Approaches to 3D periodic attractor when $\tau = 9.5$. **(d)** Time series when $\tau = 9.5$. **(e)** Approaches to 3D periodic attractor when $\tau = 10$. **(f)** Time series when $\tau = 10$. **(g)** Approaches to 3D periodic attractor when $\tau = 10.5$. **(h)** Time series when $\tau = 10.5$.

Moreover, for the data set (49) with $b = 0.1$, and $c = 0.1$, it is observed that increasing the value of τ causes transfers the dynamics behavior from E^* to a chaotic attractor as shown in Figure (14).

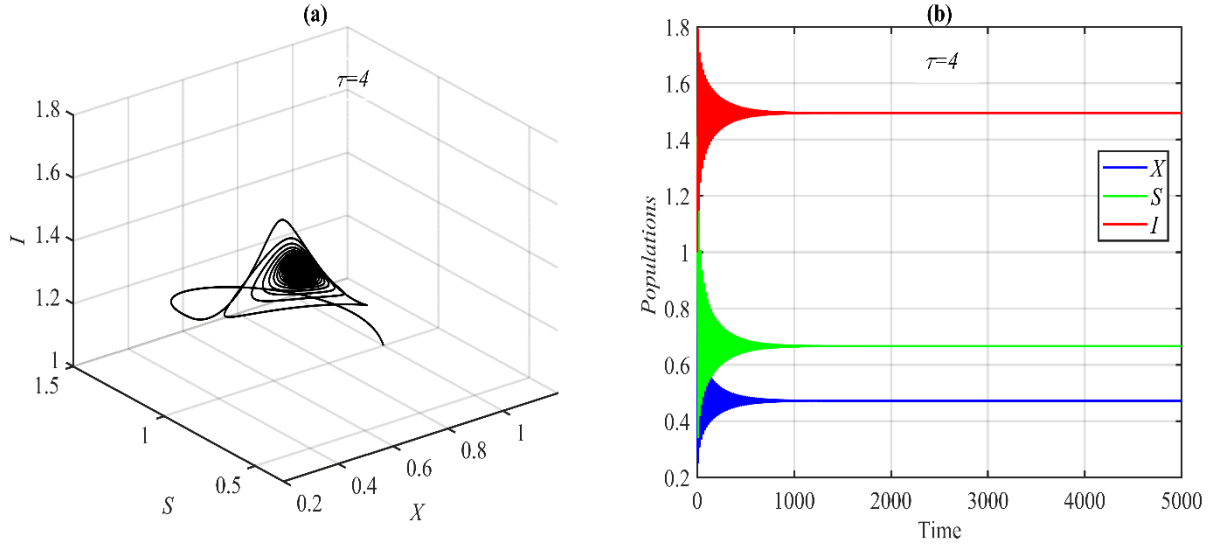

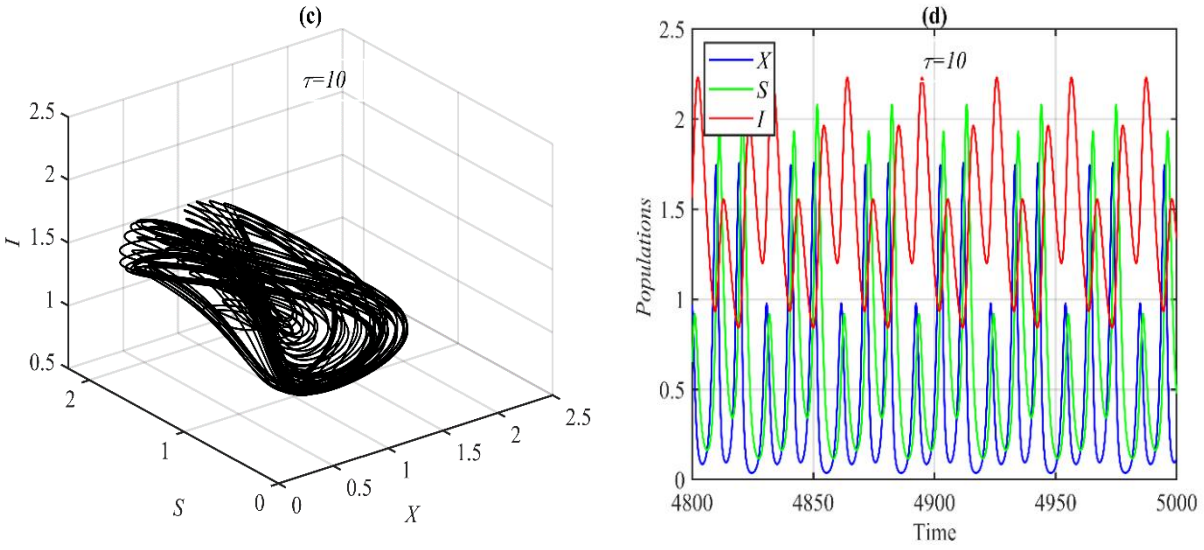

Fig. 14: The phase portraits and their time series of system (1) utilizing data set (49) with $b = 0.1$, and $c = 0.1$ and different values of τ. **(a)** Approaches to $E^* = (0.47,0.66,1.49)$ when $\tau = 4$. **(b)** Time series when $\tau = 4$. **(c)** chaotic attractor when $\tau = 10$. **(d)** Time series when $\tau = 10$.

9. CONCLUSIONS

The impact of fear and hunting cooperation on the dynamics of a delayed prey-predator system with predator sickness is theoretically stated and then examined analytically and numerically in this work. The Lotka-Volterra functional response depicts the change of food from prey to predator. Due to the incubation period, it is thought that there is a time lag between becoming infected after interaction between susceptible and infected predator individuals. The suggested system contains at most four nonnegative equilibrium points, as observed. The stability analysis around them is examined in two cases: when $\tau = 0$ and when $\tau > 0$. It is explored whether Hopf bifurcation can occur around the inner positive equilibrium point. Furthermore, the center manifold theorem was used to examine the direction and stability of the bifurcation periodic dynamics. Finally, a thorough numerical analysis was performed to comprehend the impact of factors on the system's dynamics.

The following conclusions are drawn from the numerical simulation. The fear rate has a stabilizing effect on the suggested system's dynamics. The delay, on the other hand, has a

destabilizing influence on the dynamics of the suggested system. The hunting cooperation rate has a destabilizing influence on the dynamics of the system (1) until a certain value is reached, at which point the infected predator dies. All of the system's mortality rates (1) have an extinction effect on the system. The growing intrinsic growth rate of the prey species has a coexistence impact on the system (1) dynamics, and the system becomes stable at the positive equilibrium point up to a vital value before losing stability and undergoing a Hopf bifurcation. In contrast, the rising intraspecific competition rate stabilizes the system at the coexistence equilibrium point up to a vital value, and then it is causing the system species to gradually extinction. Finally, the conversion rate of prey biomass into predator biomass (similar to the infection rate) generates system persistence, and the solution is stable at the positive equilibrium point.

CONFLICT OF INTERESTS

The author(s) declare that there is no conflict of interests.

REFERENCES

[1] R.M. Anderson, R.M. May, Population biology of infectious diseases: Part I, Nature. 280 (1979), 361-367. https://doi.org/10.1038/280361a0.

[2] H.W. Hethcote, W. Wang, L. Han, Z. Ma, A predator–prey model with infected prey, Theor. Popul. Biol. 66 (2004), 259-268. https://doi.org/10.1016/j.tpb.2004.06.010.

[3] M. Haque, J. Zhen, E. Venturino, An ecoepidemiological predator-prey model with standard disease incidence, Math. Meth. Appl. Sci. 32 (2009), 875-898. https://doi.org/10.1002/mma.1071.

[4] A.M. Bate, F.M. Hilker, Complex dynamics in an eco-epidemiological model, Bull. Math. Biol. 75 (2013), 2059-2078. https://doi.org/10.1007/s11538-013-9880-z.

[5] S. Jana, S. Guria, U. Das, et al. Effect of harvesting and infection on predator in a prey-predator system, Nonlinear Dyn. 81 (2015), 917-930. https://doi.org/10.1007/s11071-015-2040-2.

[6] A.S. Abdulghafour, R.K. Naji, A study of a diseased prey-predator model with refuge in prey and harvesting from predator, J. Appl. Math. 2018 (2018), 2952791. https://doi.org/10.1155/2018/2952791.

[7] I.M. Bulai, F.M. Hilker, Eco-epidemiological interactions with predator interference and infection, Theor. Popul. Biol. 130 (2019), 191-202. https://doi.org/10.1016/j.tpb.2019.07.016.

[8] K.Q. AL-Jubouri, R.M. Hussien, N.M.G. Al-Saidi, Modeling of an eco-epidemiological system involving various epidemic diseases with optimal harvesting, Eurasian J. Math. Computer Appl. 8 (2020), 4-27. https://doi.org/10.32523/2306-6172-2020-8-2-4-27.

[9] H.A. Ibrahim, R.K. Naji, A prey-predator model with Michael Mentence type of predator harvesting and infectious disease in prey, Iraqi J. Sci. 61 (2020), 1146-1163. https://doi.org/10.24996/ijs.2020.61.5.23.

[10] M. Hossain, N. Pal, S. Samanta, Impact of fear on an eco-epidemiological model, Chaos Solitons Fractals. 134 (2020), 109718. https://doi.org/10.1016/j.chaos.2020.109718.

[11] S. Zhang, S. Yuan, T. Zhang, Dynamic analysis of a stochastic eco‐epidemiological model with disease in predators, Stud. Appl. Math. 149 (2022), 5-42. https://doi.org/10.1111/sapm.12489.

[12] A.P. Maiti, C. Jana, D.K. Maiti, A delayed eco-epidemiological model with nonlinear incidence rate and Crowley–Martin functional response for infected prey and predator, Nonlinear Dyn. 98 (2019), 1137-1167. https://doi.org/10.1007/s11071-019-05253-6.

[13] S. Samanta, P.K. Tiwari, A.K. Alzahrani, A.S. Alshomrani, Chaos in a nonautonomous eco-epidemiological model with delay, Appl. Math. Model. 79 (2020), 865-880. https://doi.org/10.1016/j.apm.2019.11.006.

[14] R.M. Hussien, R.K. Naji, The dynamics of a delayed ecoepidemiological model with nonlinear incidence rate, J. Appl. Math. 2023 (2023), 1366763. https://doi.org/10.1155/2023/1366763.

[15] S. Biswas, S.K. Sasmal, S. Samanta, et al. Optimal harvesting and complex dynamics in a delayed eco-epidemiological model with weak Allee effects, Nonlinear Dyn. 87 (2016), 1553-1573. https://doi.org/10.1007/s11071-016-3133-2.

[16] X. Meng, F. Li, S. Gao, Global analysis and numerical simulations of a novel stochastic eco-epidemiological model with time delay, Appl. Math. Comput. 339 (2018), 701-726. https://doi.org/10.1016/j.amc.2018.07.039.

[17] J. Liu, B. Liu, P. Lv, T. Zhang, An eco-epidemiological model with fear effect and hunting cooperation, Chaos Solitons Fractals. 142 (2021), 110494. https://doi.org/10.1016/j.chaos.2020.110494.

[18] U. Ghosh, A.A. Thirthar, B. Mondal, et al. Effect of fear, treatment, and hunting cooperation on an eco-epidemiological model: memory effect in terms of fractional derivative, Iran. J. Sci. Technol. Trans. A. Sci. 46 (2022), 1541–1554. https://doi.org/10.1007/s40995-022-01371-w.

[19] N. Sk, P.K. Tiwari, S. Pal, A delay nonautonomous model for the impacts of fear and refuge in a three species food chain model with hunting cooperation, Math. Computers Simul. 192 (2022), 136-166. https://doi.org/10.1016/j.matcom.2021.08.018.

[20] N.H. Fakhry, R.K. Naji, The dynamics of a square root prey-predator model with fear, Iraqi J. Sci. 61 (2020), 139-146. https://doi.org/10.24996/ijs.2020.61.1.15.

[21] S. Biswas, P.K. Tiwari, S. Pal, Delay-induced chaos and its possible control in a seasonally forced eco-epidemiological model with fear effect and predator switching, Nonlinear Dyn. 104 (2021), 2901-2930. https://doi.org/10.1007/s11071-021-06396-1.

[22] S.X. Wu, X.Y. Meng, Dynamics of a delayed predator-prey system with fear effect, herd behavior and disease in the susceptible prey, AIMS Math. 6 (2021), 3654-3685. https://doi.org/10.3934/math.2021218.

[23] F.H. Maghool, R.K. Naji, The dynamics of a tritrophic Leslie-Gower food-web system with the effect of fear, J. Appl. Math. 2021 (2021), 2112814. https://doi.org/10.1155/2021/2112814.

[24] H.A. Ibrahim, D.K. Bahlool, H.A. Satar, et al. Stability and bifurcation of a prey-predator system incorporating fear and refuge, Commun. Math. Biol. Neurosci. 2022 (2022), 32. https://doi.org/10.28919/cmbn/7260.

[25] J.K. Hale, Functional differential equations, Springer, New York, 1971.

[26] K. Sarkar, S. Khajanchi, P.C. Mali, A Delayed Eco-Epidemiological Model with Weak Allee Effect and Disease in Prey, Int. J. Bifurcation Chaos. 32 (2022), 2250122. https://doi.org/10.1142/s021812742250122x.

[27] B.D. Hassard, N.D. Kazarinoff, Y. Wan, Theory and applications of Hopf bifurcation, London Math. Soc. Lecture Note Ser, vol 41. Cambridge University Press, Cambridge, (1981).

[28] R.K. Goodrich, A Riesz representation theorem, Proc. Amer. Math. Soc. 24 (1970), 629-636.